5-2009

The Role of Notch Signaling in Neurotransmitter Phenotype Specification in Xenopus Laevis

Michael S. Harper
College of William and Mary

Follow this and additional works at: https://scholarworks.wm.edu/honorstheses

The Role of Notch Signaling in Neurotransmitter Phenotype Specification in
Xenopus laevis

A thesis submitted in partial fulfillment of the requirement
for the degree of Bachelors of Science in **Neuroscience** from
The College of William and Mary

by

Michael S. Harper
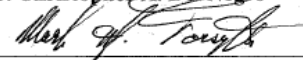
Accepted for ___HONORS_____
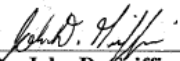
_____
Dr. Margaret S. Saha, Advisor

_____
Dr. Christopher A. Del Negro

_____
Dr. Mark H. Forsyth

_____
Dr. John D. Griffin

Williamsburg, VA
May 7, 2009

i

Acknowledgments
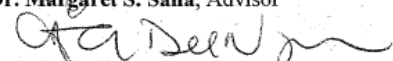
I would like to gratefully acknowledge Matt Wester, Rebecca Lowdon, and all the members of the Saha lab for advice, assistance, and engaging discussions. I would also like to thank my family for supporting me, and the members my committee. Most of all I would like to thank Dr. Margaret Saha, not only for mentoring me during this project but for providing me with the opportunity to do undergraduate research.

Table of Contents

List of Figures

Abstract

The development of a functional nervous system depends on individual neurons acquiring an appropriate neurotransmitter phenotype. In the developing spinal cord, neurons often display different fates in a "salt and pepper" pattern, and the mechanism by which this non-random dispersed patterning occurs remains largely unknown. However, given the role of Notch signaling in neurogenesis, the Notch pathway is a possible mediator because of its role in lateral inhibition. We hypothesized that Notch signaling is involved in the decision between GABAergic and glutamatergic fates and that activating Notch signaling *in vivo* would result in more neurons acquiring a glutamatergic neurotransmitter phenotype, while inactivating Notch signaling would increase GABAergic phenotypes. To test this hypothesis, we activated Notch signaling by injecting mRNA for X-Notch ICD and inactivated Notch signaling by injecting mRNA for xSu(H) DNA Binding Mutant, an inactive form of the transcription factor xSu(H). Embryos injected with X-Notch ICD lacked expression of the glutamate transporter *xVGlut1* and the GABA transporter *xGAT1,* and embryos injected with xSu(H) DBM showed widespread ectopic expression of neuronal marker *xNBT* and *xVGlut1*. Embryos did not show ectopic expression of *xSlug*, suggesting that ectopic cells were not derived from the neural crest. HNK-1 immunohistochemistry showed ectopic expression in what appeared to be aberrant neural processes, indicating that the ectopic cells may be differentiated neurons or glia. We are now attempting to activate inducible xSu(H) DBM-GR and X-Notch ICD-GR at different developmental stages to determine the later effects of Notch activation, and if ectopic expression only occurs during a certain window of competency.

Introduction

Neurotransmitter phenotype specification, the process by which neurons are instructed to express proteins for the use of specific chemical messengers, is a necessary step in the development of a functional nervous system. Understanding neurotransmitter phenotype specification is a complex problem because there are a significant number of genes that a neuron must coordinately express to be able to use a specific neurotransmitter. For example, the expression of genes for enzymes that synthesize a neurotransmitter must be co-regulated with the expression of genes for transport proteins for the same neurotransmitter. Moreover, there are no neurotransmitter phenotype specification programs that are common to all neurons of a specific phenotype; conversely, any given program may be necessary for multiple phenotypes (Goridis and Rohrer, 2002). To add to the complexity of neurotransmitter phenotype specification, there is no single gene that has been found to be uniquely employed for one neurotransmitter phenotype as part of the specification process. The need for coordinated expression of neurotransmitter-specific genes with programs for axon guidance further adds to the complexity (Goridis and Brunet, 1999).

The more that is understood about neurotransmitter phenotype specification, the greater the potential to manipulate developmental programs for use in clinical applications such as cell replacement therapies for neurodegenerative diseases (Sasai *et al*., 2008). While there are many aspects of neurotransmitter phenotype specification that are not yet understood, my focus will be on one particular aspect: the acquisition of different neurotransmitter phenotypes in neighboring cells. The Notch signaling pathway,

the focus of this research, is active early in development and functions via cell contact signaling, and may account for differences in neurotransmitter phenotype at the cell-to-cell level.

Components of Neural Development

In *Xenopus laevis*, a model system for early development, neural development begins when the neurectoderm is specified during gastrulation by the inhibition of Bone Morphogenetic Proteins (BMPs). BMPs are members of the Transforming Growth Factor-β (TGF-β) family and are secreted by the mesoderm (DeRobertis and Kuroda, 2004). When the mesoderm involutes, BMPs induce a non-neural fate in the regions of the ectoderm that lack BMP inhibitors. BMP inhibitors include Noggin and Chordin, which bind directly to BMPs, and Follistatin, which trimerizes with BMPs and the BMP receptor (Weinstein and Hemmati-Brivanlou, 1999). The induction of neural tissue by inhibition of BMPs has led to the neural-by-default hypothesis, which proposes that once ectoderm is established, no additional signals are necessary for neuralization. The expression of the early neural marker SoxD before gastrulation supports this hypothesis (Chitnis, 1999), but neuralizing factors that are independent of BMP inhibition have also been identified (Harland, 2000).

Wnt inhibition, fibroblast growth factor (FGF) signaling, and Smad 10 expression have shown been to cause neuralization independent of BMP activity (Weinstein and Hemmati-Brivanlou, 1999). FGF signaling can induce neuralization in dissociated animal caps and appears to be required for neuralization in animal caps *in vivo*. Smad 10 induces neuralization despite functional assays that indicate it does not antagonize BMP signaling

from the mesoderm. Wnt inhibition is also necessary for formation of the neurectoderm, since Wnt inhibitors such as FrzB and dickkopf are necessary for cephalization by specifying the anterior neural plate.

Transient calcium activity has been proposed as an additional mechanism in regulating the epidermal versus neural cell fate decision (Leclerc *et al*., 2006). Dissociation of animal caps in calcium and magnesium free solution causes neuralization by causing Ca^{2+} ions to be released from internal stores in response to the inverted concentration gradient. Neuralization is blocked when dissociated animal cap cells were loaded with the Ca^{2+} chelator BAPTA, indicating that the increase in intracellular Ca^{2+} is necessary for neuralization.

Subsequent patterning of the neural plate is determined by the expression of proneural genes and genes that prevent neuronal differentiation (Chitnis, 1999). In *Xenopus*, primary neurogenesis is limited to three pairs of lateral stripes that express neurogenin (Xngnr-1), an ortholog to the *Drosophila* proneural gene atonal (Sasai, 1998). The neurogenic stripes of the neural plate are bordered by Zic2, a zinc-finger transcription factor, which is expressed in the remaining neurectoderm and perhaps regulates the size and positions of the stripes (Chitnis, 1999). Xngnr-1 leads to the activation of the proneural gene Xath-3, which is another ortholog to atonal, and the neurogenic gene X-Delta-1.

Xngnr-1 expression within the lateral stripes is modulated by Notch signaling (Chitnis, 1999). X-Delta-1 activates X-Notch on adjacent cells, which causes a decrease in Xngnr-1 expression in a process of lateral inhibition. Low levels of Xngnr-1 prevent cells from differentiating into neurons and high levels activate expression of proneural

genes that eventually lead to the expression of NeuroD, a neuronal terminal differentiation gene (Lee *et al.,* 1995).

Neural crest, which lies between the neural and non-neural ectoderm, gives rise to a diverse array of cell types including the neurons and glia of the peripheral nervous system in *Xenopus* (Bronner-Fraser and Fraser, 1988). Wnt, BMP, and FGF signals from the neural folds and the non-neural ectoderm induce neural crest at the time of neural plate formation (Barembaum and Bronner-Fraser, 2005). BMP4 over-expression reduces the size of the neural plate, and expression of BMP antagonists has the opposite effect. The strongest inducer of neural crest may be the Wnt family proteins, since Wnt1 has been shown to induce neural crest in chick in the absence of other inducing factors, and several Wnt family members in *Xenopus* can induce neural crest in neuralized animal caps. Induction of the neural crest activates the expression of neural crest determinants slug (Mayor *et al.*, 1995) and FoxD3 (Kos *et al*., 2001).

The neural folds, which bend and fold during *Xenopus* neural tube closure to become the dorsal neural tube, contain the neural crest cells. The cells of the dorsal neural tube express BMP, which is involved in dorsal-ventral patterning by creating opposing gradients with Sonic Hedgehog (SHH) proteins secreted from the ventrally located notochord (Briscoe and Novitch, 2007). The SHH/BMP concentration gradient drives differential expression of transcription factors, which leads to different cell types on the dorsal-ventral axis. Following neural tube closure, neural crest cells transition from epithelial to mesenchymal and migrate away from the neural tube.

The *Xenopus* embryonic spinal cord consists of a diverse array of cell types, including radial glia (Messenger and Warner, 1989), six major classes of spinal cord

neurons (Roberts 2000), and undifferentiated cells such as the neural crest stem cells, oligodendrocyte precursors, and secondary neuron precursors. The mechanisms of neural development from the time of neural induction to SHH/BMP signaling explain how regions of neural tissue are defined, but are insufficient in explaining how specification occurs between these adjacent cells. It has been proposed that calcium activity is a mechanism by which individual cells can become specified (Gu and Spitzer, 1997). Neurons are switched to express an inappropriate neurotransmitter when their Ca^{2+} activity is modified, indicating that calcium activity specifies the neurotransmitter phenotypes of neurons. Artificially increased Ca^{2+} activity causes an increase in inhibitory neurotransmitter phenotypes and a decrease in excitatory phenotypes. Decreased Ca^{2+} activity has the opposite effect, suggesting that the effect is a homeostatic mechanism for regulating for the amount of excitation and inhibition in neural networks.

A promising candidate mechanism that could account for differences at the cell-to-cell level is the Notch signaling pathway, a highly conserved mediator of signaling between adjacent cells (Beatus and Lendahl, 1998). Notch signaling is involved in many cell fate decisions, the first of which in *Xenopus* appears to be the initial lateral inhibition of Xngnr-1 expression in the lateral stripes of the neural plate. The Notch protein, originally found in *Drosophila*, is a transmembrane receptor activated by the ligands Delta and Serrate that are located on the membranes of adjacent cells (Artavanis-Tsakonas *et al.,* 1999). Cell-to-cell signaling provides a mechanism that can produce finely tuned differentiation of neighboring cells, and the Notch signaling pathway is the only known embryonic signaling pathway based on cell-to-cell contact.

The Notch Signaling Pathway

Notch signaling has been the focus of considerable attention during the last twenty years because of its unique mechanism of lateral inhibition, by which differentiating cells prevent neighboring cells from adopting similar fates (Beatus and Lendahl, 1998). Moreover, the structure and function of the Notch protein is highly conserved across vertebrates and invertebrates, is almost ubiquitously involved in cell fate decisions of many different tissues throughout development, and has been implicated in human diseases (Ellisen *et al.,* 1991, Li *et al.,* 1997, Garg *et al.,* 2005).

A notched-wing phenotype caused by haploinsufficiency of the *Notch* locus was among the first genetic variations observed in *Drosophila* (Louvi and Artavanis-Tsakonas, 2006). It was later found that Notch is responsible for segregating prospective neural cells from prospective epidermal cells (Poulson, 1940) and is a transmembrane receptor protein (Wharton *et al.,* 1985). Experiments in insects showed that segregation of neural and epidermal fates by Notch functions via lateral inhibition; when individual neuroblasts were ablated, neighboring cells that would normally become epidermal became neuroblasts instead (Doe and Goodman, 1985). The mechanism of lateral inhibition, in which cells prevent their neighbors from adopting the same fate through ligands and receptors located on adjacent cell membranes, is responsible for the surge in Notch research because this type of mechanism can explain how otherwise equivalent groups of cells become further differentiated (Louvi and Artavanis-Tsakonas, 2006).

A Notch ortholog in *Xenopus* was first found by screening a *Xenopus* cDNA library with *Drosophila* Notch DNA (Coffman *et al.,* 1990). Characterization of the

Xenopus ortholog of Notch revealed a protein similar in structure and developmental expression to *Drosophila* Notch, suggesting that lateral inhibition was involved in cell fate decisions in vertebrates as well as insects.

Coffman and colleagues (Coffman *et al.,* 1993) first characterized the effects of Notch signaling in *Xenopus* and proposed the idea that Notch regulates between two potential fates by inhibiting cell fate commitment. The researchers created a deletion construct of Notch by truncating the extracellular domain and injected the deletion construct mRNA into early cleavage stage embryos. The deletion construct constituted active Notch, since it lacked the extracellular domain of the Notch protein, which normally binds the intracellular domain (ICD) to the membrane, and Notch ICD affects gene transcription only when it is released from the membrane. Activation of Notch by expression of the deletion construct resulted in hypertrophy of neural and mesodermal tissues, with concomitant reduction of epidermal and neural crest tissues.

Cell division in experimental embryos was blocked to determine if the cause of hypertrophy was stimulated cell division in neural and mesodermal tissues or the conversion of cells that would normally become epidermal and neural crest derivatives into neural and mesodermal derivatives. Manipulated embryos were treated with hydroxyurea and aphidicolin (HUA), which blocks DNA synthesis and arrests the cell cycle (Harris and Hartenstein, 1991). The neural and mesodermal derivatives overgrew even in the absence of cell division, indicating that hypertrophy was not caused by increased cell division.

This disagreed with results of *Drosophila* experiments; here an active Notch construct caused neural hypertrophy, but inhibited Notch in *Drosophila* produced the

same effect. The authors proposed that Notch does not provide instructive signals, but rather delays differentiation. This hypothesis was supported because animal caps dissected from Notch-activated embryos responded more strongly to neural inductive signals and had extended competence to respond to neural signals. This suggests that cells that would normally differentiate into non-neural cells were being prevented from doing so, increasing the total number of cells that would respond to a neural inducer. The authors suggest that since Notch activation by mRNA injection is temporary, it is possible that animal caps responded to neural inducers only when levels of active Notch dropped.

This experiment demonstrated that timing is key to the effects of lateral inhibition on cell fate decisions, since preventing differentiation while neural inducing factors are present blocks neuronal differentiation. Normally, Notch signaling is transient and levels of free Notch ICD drop at a time when neural crest inducing factors are present, causing the cells to differentiate into neural crest cells. Hypertrophy of neural tissues in up-regulated Notch embryos may have been caused when cells with activated Notch missed the window of opportunity to become neural crest, becoming neural instead when levels of active Notch dropped. Normal Notch signaling may be more transient than up-regulated Notch signaling since it allows for the specification of neural crest cells. Orthologs for two ligands of Notch, Delta and Serrate, are conserved between *Drosophila* and *Xenopus*. An ortholog of the *Drosophila* gene Delta, a transmembrane protein with extracellular epidermal growth factor-like (EGF) repeats (Beatus and Lendahl, 1998), was cloned using polymerase chain reaction and characterized in *Xenopus*. Expression of X-Delta-1 prefigures the expression of neuronal markers, suggesting that X-Delta-1 is

expressed in prospective neurons. Expression of the ligand in presumptive neurons indicates that neurons laterally inhibit adjacent cells from also becoming neurons through Notch activation (Chitnis *et al.,* 1995). This is consistent with Notch activity in *Drosophila*, where neuroblasts prevent adjacent cells from adopting the same fate.

Functional assays of X-Delta-1 showed that up-regulation of X-Delta-1 inhibited primary neurogenesis and down-regulation resulted in a neurogenic phenotype (Chitnis *et al.,* 1995). These results confirm the effects of lateral inhibition in preventing neuronal differentiation. The proposed mechanism is that neural inducing factors cause some cells to begin differentiating into neurons, which then begin to express X-Delta-1. Cells that express X-Delta-1 activate Notch on adjacent cells and prevent them from also differentiating into neurons. When X-Delta-1 is inactivated, the neighboring cells differentiate into neurons instead of remaining uncommitted.

The major downstream effectors of Notch signaling in *Xenopus* are orthologs of the *Drosophila* Enhancer of Split Complex [E(spl)-C]. Enhancer of Split Related-1 (ESR-1) is a bHLH-WRPW protein that is expressed in regions of primary neurogenesis. ESR-1 is induced by overexpression of X-Delta-1 and by an activated form of Notch (Chitnis *et al.* 1995), suggesting that ESR-1 expression is positively regulated by Notch. The control of ESR-1 by Notch and its anti-neural effects confirm that the mechanism by which Notch prevents neuronal differentiation is conserved between insects and vertebrates. The mediator by which Notch regulates ESR-1 was found to be an ortholog of the mediator in *Drosophila*, Suppressor of Hairless (Su(H)). XSu(H) was isolated and shown to bind both to DNA and to X-Notch ICD. Moreover, xSu(H) drove expression of ESR-1

when fused to ankyrin repeats, which mimic the effects of Notch ICD binding (Wettstein *et al.,* 1997).

The basic proteins involved in the standard Notch signaling pathway in vertebrates have been reviewed here. To summarize, the conventional model begins with Notch receptor activation by the ligand Delta, which allows the ICD of Notch to be cleaved. Free Notch ICD subsequently dimerizes with Su(H), forming an active transcription factor that drives expression of genes that suppress proneural genes and inhibit differentiation.

The Role of Notch in Neural Development

The effects of Notch activation on gene expression further downstream of ESR-1 are poorly understood. Identifying the role of Notch is complicated by the multitude of temporally and spatially distinct Notch signaling events throughout early development and the plurality of downstream effectors (Morrison *et al.*, 2000, Cornell and Eisen 2000, 2002). The range of cell fate decisions that Notch regulates is still unclear, and it is still unknown whether transient Notch activation permanently alters the competence of a cell or only passively delays differentiation.

Notch has been shown in chick to switch neural crest stem cells from neurogenesis to gliogenesis irreversibly, indicating that Notch can act instructively (Morrison *et al.*, 2000). Activation of Notch signaling in cultured neural crest stem cells severely decreased the neurogenic capacity of the cells. When Notch-activated neural crest stem cells were challenged with BMP2, a strong neurogenic factor later in development, they did not undergo neuronal differentiation. Even transient Notch

activation caused neural crest stem cells to lose their neurogenic capacity, suggesting that Notch signaling acts instructively, in contrast to the apparently restrictive signaling seen *in vivo* in *Xenopus* (Coffman *et al.,* 1993). The authors of the chick experiments propose that Notch signaling acts instructively in certain signaling events and restrictively in others (Morrison *et al.*, 2000).

In zebrafish, Notch signaling has been shown to regulate between a specific type of primary neuron, Rohon-Beard sensory neurons, and neural crest cells (Cornell and Eisen, 2000). Rohon-Beards are among the earliest born neurons (Lamborghini, 1980) and their precursors are intermingled with pre-migratory neural crest cells in the lateral neural plate boundary. The proximity of these cells indicates that Notch signaling may be necessary to determine cell fate specification. Embryos with a genetic loss-of-function mutation in DeltaA, the zebrafish homolog of Delta, have supernumerary Rohon-Beard neurons in the spinal cord and a concomitant decrease in trunk neural crest derivatives. When prospective Rohon-Beard cells undergo differentiation in response to the initial neurogenic cues, they express DeltaA, which prevents adjacent cells from also becoming Rohon-Beards. In normal signaling, Notch-activated cells appear to remain undifferentiated long enough to receive inductive cues to become neural crest.

A downstream component of the Notch signaling pathway in zebrafish is responsible for the cell fate decision between Rohon-Beard neurons and neural crest cells. Zebrafish neurogenin-1 (Ngn-1) is expressed in the lateral neural plate, where pre-Rohon-Beard and pre-neural crest cells are present. High Ngn-1 levels are necessary to form Rohon-Beard neurons. Notch signaling represses Ngn-1, and this suppression is necessary for the specification of neural crest cells (Cornell and Eisen, 2002). Since low

Ngn-1 levels alone do not specify neural crest cells, Notch signals are restrictive in this decision. Ngn-1 may interact on both ends of the Notch signaling pathway: it may drive expression of Delta in prospective Rohon-Beard cells, and Su(H) down regulates its expression.

The Role of Notch in Neurotransmitter Phenotype Specification

Despite the recent surge in Notch signaling research, the downstream effects of transient Notch activation in vertebrates remain poorly understood. However, there is preliminary evidence that Notch signaling may affect the specification of neurotransmitter phenotype. Inhibition of human hairy/enhancer of split (HES-1), a human ortholog of [E(spl)-C], in human neural stem cells increased expression of neuronal markers (Kabos *et al.,* 2002). In un-manipulated cultures of neural stem cells only 5-15% became neuronal; in cultures with HES-1 knocked out, approximately 80-90% of cells became neuronal. Moreover, in HES-1 knockout cultures 50-95% of cells became GABAergic, compared to 1-15% in controls. There was no difference in the number of cholinergic cells between knockouts and controls, suggesting that Notch restricts the number of cells that become GABAergic but does not regulate cholinergic differentiation.

In the *Xenopus* spinal cord, dopaminergic neurons are spaced in a non-random dispersed pattern (Heathcote and Chen, 1993, 1994), which is consistent with patterns created by lateral inhibition. In *Xenopus*, Notch has been shown to regulate dopaminergic spinal cord neuron specification. Injection of a constitutively active Notch increased the distance between dopaminergic neurons on the anterior-posterior axis (Binor and

Heathcote, 2005). The patterning of primary dopaminergic neurons in the spinal cord had been described and the distances between these neurons were found to be consistent (Heathcote and Chen, 1994). Additionally, no consistent distances between dopaminergic neurons and any other cell types were found, suggesting the presence of a mechanism that limits the formation of dopaminergic neurons in close proximity to each other. The researchers proposed that lateral inhibition through Notch signaling could be this mechanism. When the deletion construct that was developed by Coffman and colleagues (1993) was injected into one blastomere of two-cell stage embryos, fewer cells showed tyrosine hydroxylase immunoreactivity. Dopaminergic neurons that form during secondary neurogenesis, however, were unaffected. Since the presence of the deletion construct is temporary, it cannot be determined from this data if Notch signaling is involved in dopaminergic specification during secondary neurogenesis, since the active Notch construct had likely degraded prior to this time.

These results show that Notch seems to restrict two types of neurotransmitter phenotypes, since more GABAergic neurons are induced when Notch is inhibited and fewer dopaminergic neurons are induced when it is activated. It is still unclear whether Notch signaling conversely promotes the adoption of any specific neurotransmitter phenotypes, or if it only functions by restriction of potential phenotypes. However, neurons that occupy positions similar to dopaminergic neurons on the dorsal-ventral axis have different neurotransmitter phenotypes (Roberts, 2000). Cell-to-cell signaling may be necessary for the specification of the diverse cell types that are in close contact in the embryonic spinal cord.

Conclusion and Overview of Proposed Experiments

Based on the evidence presented in the primary literature, it appears that Notch signaling may be involved in neurotransmitter phenotype specification. GABAergic and glutamatergic neurons, which represent the main inhibitory and excitatory phenotypes of the CNS, can be found adjacent to each other in the neural tube, and the unique mechanism of the Notch signaling pathway may be necessary for this close specification.

Generalized from the results of Notch inhibition in human neural stem cells, our working hypothesis is that that Notch signaling regulates the decision between the specification of GABAergic and glutamatergic fates. This hypothesis leads to the prediction that inhibition of Notch signaling *in vivo* in *X. laevis* will result in an increase in the number of GABAergic neurons with a concomitant decrease in the number of glutamatergic neurons. Conversely, if Notch signaling acts instructively, then it is predicted that Notch activation will result in an increase in glutamatergic neurons and fewer GABAergic neurons.

To test this hypothesis, the Notch signaling pathway will be activated by unilateral injection of mRNA for Notch ICD (Chitnis *et al.* 1995) into 2-cell stage *X. laevis* embryos. GABAergic and glutamatergic neurons will be identified by *in situ* hybridization using antisense mRNA probes for the *X. laevis* GABA transporter, *xGAT1*, and the *X. laevis* glutamate transporter, *xVGlut1*. Antisense mRNA probes for *X. laevis* neural-β-tubulin, *xNBT*, will be used to identify all types of neurons. The effect of inhibiting Notch signaling *in vivo* will be tested by unilateral injection of a Su(H) DNA binding mutant (Su(H) DBM, Wettstein *et al.,* 1997), which causes a dominant negative

knockout of Notch signaling. Embryos will then be assayed for the expression of various

phenotype markers as outlined above.

Materials and Methods

Animals and Embryos

Adult *Xenopus laevis* frogs were purchased from Xenopus I (Ann Arbor,

Michigan), Xenopus Express (Brooksville, Florida), or Nasco. Embryos were obtained by

inducing natural mating with human chorionic gonadotropin according to the protocol

described in Sive *et al.* (2000), with minor modifications (600 units of hCG were used for

female and 400 units for male). Fertilized oocytes were dejellied in 2% L-cysteine in

0.1X Marc's Modified Ringer's (MMR) solution adjusted to pH 8.0. Following

dejellying, embryos were washed twice in 0.1X MMR and then transferred to glass

dishes containing 50-75 ml of 0.1X MMR, with 50 μg/μl gentamycin, at a density of 100-

200 embryos per plate. Dead embryos and unfertilized oocytes were removed from the

plates. Embryos that were at the two-cell stage were selected for microinjections.

Plasmid Isolation

Genes of interest that were used to synthesize sense mRNA for microinjections or

antisense probes for *in situ* hybridization had been ligated into various plasmid vectors

and transformed into various E. coli hosts (Tables 1.2, 2). Plasmids were amplified by

incubating 10 μl of -20°C bacterial culture glycerol stock in 150 ml of LB for 12-18

hours in a 37°C shaking incubator. Plasmids were isolated using a midiprep DNA isolation kit (Biorad) according to the manufacturer's instructions. Purity and identity of isolated plasmid was assessed by restriction endonuclease digest and agarose mini-gel electrophoresis. Restriction digests were assembled in a 1.5 ml sterile microcentrifuge tube with 12.5 μl sdd H_2O, 2 μl of the appropriate 10X buffer (Promega), 5 μl template DNA (200 ng/μl), and 0.5 μl restriction enzyme (10 U/μl). Amounts were scaled appropriately based on the concentration of the plasmid DNA so that 1 μg of DNA was digested (final concentrations 1X buffer, 0.05μg/μl template DNA, 0.25U/μl restriction enzyme). Digests were incubated for 1-2 hours at 37°C, then 4 μl of 6X DNA loading dye was added and the entire volume was run on an agarose mini-gel. Agarose mini-gels were assembled by dissolving 0.6 g agarose in 50 ml 1X Tris Acetate EDTA (TAE), for a concentration of 1.2% agarose, and microwaving the mixture on "high" for 90 seconds. Once the mixture cooled, 2.5 μl of 10 mg/ml ethidium bromide was added to the solution, for a final concentration of 0.5 μg/ml, and the solution was poured into a tray that was positioned perpendicularly in the gel box as to form an enclosed area. The gel box was filled with 1X TAE, 10 μl of 1 Kb[+] ladder (Invitrogen) was loaded into the first well as a size standard, and the 24 μl volumes of each restriction digest were loaded into individual wells. A potential of 160-170 millivolts with a current not exceeding 500 milliamps was applied to the gel box for 20-25 minutes. Gels were viewed using an ultraviolet light transilluminator and imaged using a FluorChem HD2 (Alpha Innotech) camera and annotated with FluorChem HDC software.

Linearization

Plasmids were linearized for transcription using a restriction endonuclease site that would allow for either probe synthesis in the antisense direction or capped mRNA synthesis in the sense direction. Linearizations were assembled in a 1.5 ml sterile microcentrifuge tube by combining 68 μl sdd H_2O, 10 μl appropriate 10X buffer (Promega), 20 μl plasmid DNA (1 μg/μl), and 2 μl restriction enzyme (10 U/μl, Promega) (final concentrations 1X buffer, 0.2 μg/μl plasmid DNA, 0.2 U/μl restriction enzyme). Assembled linearizations were incubated for at least 2 hours at 37°C. Protein was removed with 100 μl of phenol/chloroform:isoamyl alcohol and then 100 μl of chloroform:isoamylalcohol. Linearized DNA was then precipitated by adding 10 μl (1/10th volume) 3M sodium acetate and 220 μl (2 volumes) of 100% ethanol to the tube and placing it at -80°C for at least 20 minutes. A DNA pellet was formed by centrifuging the tube at 14,000 RPM at 4°C for 20 minutes. Supernatant was removed and the pellet was washed with 200 μl 70% ethanol and spun for 5 minutes at 4°C. Supernatant was removed and the pellet was dried for 3 minutes under vacuum suction, then re-suspended in 20 μl of 1X TE (10 mM Tris, 1 mM EDTA). Quality and concentration were evaluated by running a 1μl sample on a 1.0% agarose mini-gel and comparing the fragment size to standard size ladder.

Capped mRNA Synthesis

Capped sense mRNA for microinjection was transcribed using the Ambion mMessage mMachine SP6 kit, which adds a 7-methyl guanosine cap structure at the 5' end of the mRNA to ensure efficient translation. The manufacturer's instructions were

followed and the reactions were run for 2 hours at 37°C. Template DNA was removed by

DNAse treatment following transcription and purification was performed using the

RNEasy MinElute Cleanup kit (Qiagen). Concentration was determined by measuring a

1-µl sample in a Nanodrop spectrophotometer, and purity was determined by agarose

mini-gel electrophoresis. A 1-µl sample of mRNA was combined with 9 µl sdd H_2O and

2 µl 6X DNA; the 12-µl sample was then run out on a 1.2% agarose mini-gel as

described. The remaining mRNA was stored at -20°C until use.

Microinjections

Constitutive Construct Modifications

Perturbations of the Notch signaling were effected by injection of capped mRNA

into one blastomere of 2-cell stage embryos. In *Xenopus* embryos the initial cleavage is a

lateral division; unilateral injection causes one side of the embryo to have altered gene

expression, while the other side serves as an internal control.

Glass capillaries that were 100 microns in diameter (Drummond) were pulled

using the PUL-1 machine to a bore of 5 microns. Needle tips were clipped to a size of 20-

30 microns to produce a sharp edge and optimal size to allow for front-loading of

injection mix and accurate delivery of injection volumes. Needles were loaded onto a

Nanoject *II* (Drummond) apparatus according to the manufacturer's instructions.

Embryos were injected in batches of 40 at a time in 1/3X MMR solution with 4% ficoll.

Concentrated mRNA was diluted in nuclease-free water to a final concentration of 326

ng/µl, and 4.6 nl was injected unilaterally into one blastomere, delivering 1.5 ng of Notch

ICD or Su(H) DBM mRNA (Wettstein *et al.,* 1997) and 0.5 ng of tracer Green

Fluorescent Protein (GFP) mRNA (courtesy of Klymkowsky lab). Following injection, embryos remained in 1/3X MMR for 2 hours, and then were transferred to 0.1X MMR with 4% ficoll for 8-15 hours. Following this rest period they were transferred to 0.1X MMR and reared until the desired stages. In cases where injected mRNAs caused morphological defects that made staging difficult, stages were assessed by the age of un-injected sibling embryos, which were reared in 0.1X MMR at the same temperature. Embryos that served as injected controls were injected with 4.6 nl nuclease-free water with 0.5 ng GFP mRNA, and then reared in the same way as experimental embryos. All embryos were fixed for ISH or IHC as described.

Inducible Modifications

Microinjections of Su(H) DBM-GR and Notch ICD-GR (Wettstein *et al.,* 1997, courtesy of McLaughlin Lab) were carried out according to the same procedure as above. The injection mixes were made so that injections of 4.6 nl would deliver 1.5 ng of mRNA, along with 0.5 ng mRNA for GFP. Inducible fusion proteins were activated by transferring embryos at the desired stages (NF stages 11, 12, and 13, corresponding to different stages of gastrulation) into 0.1X MMR containing 10 μM dexamethasone. Baseline comparisons to constitutive mRNA injections were made by treating embryos with dexamethasone less than 2 hours after the injections. Dexamethasone was replenished every 24 hours while embryos were reared to the desired stages; embryos were then fixed for ISH or IHC as described.

Probe Synthesis

In situ hybridization probes (Table 1) were synthesized by assembling a transcription reaction according to standard protocol (Sambrook and Russell, 2001). A mix of 2.5 mM rNTPs was made by combining 10 µl of 10 mM rCTP, rGTP, and rATP; 6.5 µl 10 mM rUTP (Promega); and 3.5 µl 10 mM digoxigenin-11-uridine-5' triphosphate (UTP) or fluorescein-12-uridine-5' triphosphate (Roche). The transcription reaction was assembled in a 1.5 ml microcentrifuge tube by combining 10 µl 5X transcription buffer, 5 µl 0.1 M DTT (Promega), 10 µl 2.5 mM NTP mix, 20 µl nuclease free water, 3.5 µl linearized DNA (1 µg/µl), 0.5 µl RNAsin (40), and 1 µl appropriate RNA polymerase (17 U/µl) for antisense transcription (final concentrations 1X transcription buffer, 0.01 M DTT, 0.5 mM NTP mix, 0.07 µg/µl linearized DNA, 0.4 U/µl RNAsin, 0.34 U/µl RNA polymerase). The transcription reaction was run for one hour at 37°C, 1 µl appropriate polymerase was added, and transcription was run for another hour at 37°C. Probe was purified using the RNEasy Minelute RNA cleanup kit (Qiagen) according to the instructions provided with the kit. Concentrated probe was initially diluted in 300 µl ISH Buffer (50% formamide, 5X SSC, 1 mg/ml Torula RNA, 100 µg/ml heparin, 1X Dendhart's solution, 0.1% Tween 20, 0.1% CHAPS, 10mM EDTA), and further diluted by 1:10 before use in hybridization.

Gene	Length (bp)	Source	Marks…
xvGluT1	1638	Gleason *et al.,* 2003	Glutamatergic neurons
xGAT1	2451	Li *et al.,* 2006	GABAergic neurons
xNBT	841	GeneBank Accession number X15798	Neurons
xHNK-1	1651	GenBank Accession number BC082886.1 (Open Biosystems)	Neurons and Glia
xSlug	~1000	Grainger Lab	Neural Crest cells
xTH	591	Cloned in lab by RT-PCR	Dopaminergic neurons
xChat	~1600	Cloned in lab by RT-PCR	Cholinergic neurons
xSert	~1100	Cloned in lab by RT-PCR	Serotonergic neurons
xNotch ICD	2300	Wettstein *et al.,* 1997	Cells that express Notch
X-Delta-1	3156	GenBank Accession number BC070634.1 (Open Biosystem)	Cells that express Delta
xVim	540	Cloned in lab by RT-PCR	Radial Glia

Table 1.1 Summary of the genes for which antisense probes were made. The table indicates clone length, where the clone was obtained, and what the probe marks.

Gene	Plasmid	Host	Restriction Site(s)	Linearized with…	Polymerase
xVGluT1	pBSSK	DH5α	EcoRI	Not1	T3
xGAT1	pBSSK+	DH5α	EcoRI/XhoI	BamHI	T7
xNBT	pBS	DH5α	EcoRI	BamHI	T7
xHNK-1	pCMV-SPORT6	DH10B Ton A	EcoRV/NotI	EcoRI	T7
xSlug	SP72	DH5α	EcoRI	BglII	SP6
xTH	pCRII-TOPO	DH5α	EcoRI	EcoRV	SP6
xChat	pCRII-TOPO	DH5α	EcoRI	NotI	SP6
xSert	pCRII-TOPO	DH5α	EcoRI	NotI	SP6
xNotch ICD	pCS2+	Top10	EcoRI/XbaI	Cla1	T7
X-Delta-1	pCMV-SPORT6	DH5α	Sal1/Not1	EcoRI	T7
xVim	pCRII-TOPO	DH5α	EcoRI	EcoRV	SP6

Table 1.2 Summary of the genes for which antisense probes were made. The table indicates plasmid vector, host, restriction sites, and polymerase used.

Gene	Plasmid	Host	Source	Restriction Sites	Linearization Site	Polymerase
Notch ICD	pCS2+ MT	Top10	Wettstein et al 1997	EcoR1/Xba1	Not1	SP6
Su(H) DBM	pCS2+	Top10	Wettstein et al 1997	BamHI/XhoI	Not1	SP6
Notch ICD-GR	pCS2+	DH5α	Contakos et al 2005	BamHI/Xba1	Not1	SP6
Su(H) DBM-GR	pCS2+	DH5α	Contakos et al 2005	BamHI/Xba1	Not1	SP6
GFP	pCS2	DH5α	Klymkowsky Lab	Xba1/EcoR1	Not1	SP6

Table 2. Summary of the genes with which capped sense mRNA was made. The table indicates plasmid vector, host, source restriction sites, and polymerase used.

Chromogenic in situ Hybridization

Unmanipulated albino embryos that served as controls for *in situ* hybridization (ISH) were raised in 0.1X MMR and staged according to Nieuwkoop and Faber (1994). Embryos were reared to the desired stages, anesthetized with MS 222 (Sigma), and then fixed in 1X MEMFA (1X MEMFA salts, 3.7% formaldehyde, in sterile double distilled (sdd) H_2O) in 5 ml glass vials for 90 minutes to 2 hours at room temperature (RT). Fixed embryos were washed twice in 100% ethanol and then stored at -20 at 37°C in 100% ethanol.

Hybridization

Stored embryos were transferred into clean 5 ml glass vials and rehydrated over successive 5 minute washes in 75% ethanol/25% H_2O, 50% ethanol/50% H_2O, 25% ethanol/75% PTw, and 100% PTw (1X phosphate buffered saline, 0.1% Tween 20). Embryos were washed three more times for 5 minutes in PTw, then treated with 1 ml of 10 μg/ml proteinase K in sdd H_2O for 30 minutes. Embryos were treated twice for 5 minutes with 0.1M triethanolamine and acetic anhydride was added to the last 0.1M triethanolamine wash by two additions of 12.5 μl each. Embryos were re-fixed after proteinase K treatment in 4% paraformaldehyde in PTw for 20 minutes. Following re-fixation, embryos were washed three times for 5 minutes in PTw. Embryos were pre-hybridized in 500 μl ISH buffer in a 60°C shaking water bath for at least 6 hours, then 500 μl of diluted probe was added and allowed to hybridize for 8-16 hours.

Following hybridization, embryos were washed three times in 2X Standard Saline Citrate (SSC) for 20 minutes at 60°C. Embryos were treated with 20 μg/ml RNAse A in

2X SSC for 30 minutes in a 37°C water bath to eliminate unbound probe. RNAse was washed out with two 10-minute washes in 2X SSC at RT and two 30 minute washes in 0.2X SSC in a 60°C water bath. Embryos were washed twice for 15 minutes in maleic acid buffer (MAB: 10 mM maleic acid, 150 mM NaCl, pH 7.5), and then incubated for 1 hour in a solution of 2% BMB (Roche) in MAB.

The steps of *in situ* hybridization described above were also performed with the Biolane HTI automated *in situ* machine. The program "01 Day_1" was run on system 2 and used for rehydration, proteinase K treatment, triethanolamine and acetic anhydride treatment, and re-fixation. For pre-hybridization and hybridization, baskets in which embryos were contained were transferred into plastic vials, which were then placed into a 60°C shaking water bath. Following hybridization, baskets were transferred back into the jig that contained them in the machine, and the program "04 Day_2" was run on system 1 for the SSC washes, RNAse treatment, and BMB blocking. Following this program, embryos were transferred from baskets into 5 ml glass vials for the remainder of the procedure.

Following BMB blocking, antibody incubation was done with 500 μl of 1:2000 dilution of either anti-digoxigenin or anti-fluorescin antibodies conjugated to alkaline phosphatase (Sigma) at 4°C for 8-15 hours. Antibodies were washed out with five MAB washes of at least one hour each.

Color Reaction

Embryos were washed twice for 5 minutes in AP buffer (100 mM Tris, pH 9.5, 50 mM MgCl2, 100 mM NaCl, 0.1% Tween 20 (Sigma), 2 mM levamisole (Sigma)). The

color reaction was performed by incubating embryos in 1 ml AP buffer with 4.5 μl nitro-blue tetrazolium (NBT) and 3.5 μl 5-bromo-4-chloro-3-indolyl phosphate (BCIP). Color reaction times ranged from 15 minutes to 8 hours (Table 3). The color reaction was stopped by fixing embryos at 4°C for at least 8 hours in 1X MEMFA solution. Embryos were then transferred to 1X PBS and stored at 4°C until analysis.

Probe	Time
xvGluT1	3 hours
xGAT1	5 hours
xNBT	1 hour
xHNK-1	8 hours
xSlug	4 hours
xTH	5 hours
xChat	5 hours
xSert	5 hours
xNotch ICD	3:30 hours
X-Delta-1	2:30 hours
Vimentin	2 hours

Table 3. Antisense probe and time necessary to develop sufficient signal

Occasionally, pigmented embryos were used instead of albinos for microinjections. These embryos needed to have their pigment bleached so that it did not interfere with identifying signal. Color reactions in embryos that required bleaching post-*in situ* were stopped with Bouin's fixative (9.25% formaldehyde, 5% glacial acetic acid, in sdd H_2O) for 8-15 hours at 4°C. Embryos were washed twice for 5 minutes in 70% ethanol/30% PTw to clear any excess color substrates. After washes, embryos were incubated in 5 ml bleaching solution (1% H_2O_2, 5% formamide, 0.5X SSC) and placed on foil on a nutator under ultraviolet light for 1 to 2 hours, until pigment was ablated.

Whole Mount Photography

Following *in situ* hybridization, embryos in 5 ml glass vials were washed three times in 100% methanol for 10 minutes each, then placed in a glass dish containing a

solution of 2:1 benzyl benzoate: benzyl alcohol (BB:BA). Embryos were positioned using blunt forceps and pictures were taken at 30-40X magnifications against a white background. Time in light was minimized while embryos were in BB:BA solution due to a tendency for red background to form. Embryos were photographed using bright field microscopy on an Olympus SZH scope with a DP71 camera and processed with DP controller software. Contrast and color adjustments were applied to whole embryo images with Photoshop CS.

Histological Analysis

Paraffin sectioning was used to create transverse sections of embryos that had undergone *in situ* hybridization; embryos were embedded in paraffin according to a standard protocol (Sive *et al.,* 2000) with modifications and sectioned using a microtome (American Optical Company). Embryos were dehydrated by successive 15 minute washes of 100% PBS, 75% PBS/25% ethanol, 50% PBS/50% ethanol, 25% PBS/75% ethanol, and 100% ethanol. Embryos were then washed in successive 15-minute washes of 50% ethanol/50% xylene and 100% xylene. Embryos were aliquotted into individual embedding boats at this time and washed for 15 minutes in 50% xylene/50% paraffin in an oven set to 60°C. This wash was replaced with 100% paraffin and kept in the oven for 1-2 hours. Paraffin was replaced and incubated for another 1-2 hours. The last wash of paraffin was then replaced with fresh paraffin, embryos were positioned head-down for sectioning, and then allowed to cool at RT until paraffin was solid. To mount paraffin blocks to the microtome, embedding boats were peeled off of paraffin blocks, the blocks were melted to wooden chucks, and excess paraffin was removed.

Transverse sections of 10 microns were taken from head to tail using a microtome. Ribbons of paraffin sections were placed on glass slides that had been coated with a thin layer of Meyer's albumin, dried, and covered with water. When the slide was full, the water was removed and the slide was placed on a slide warmer at 35-40°C to allow sections to adhere to the slide. Excess paraffin was removed by treating slides for 5-10 minutes in Citrisolv. Slides were coverslipped using Permount toluene solution, allowed to dry overnight, and imaged using an Olympus BX60 scope with an Evolution MP color camera and QCapture software. Further color adjustments were made using Photoshop CS.

Double Fluorescent in situ Hybridization

Hybridization

The same probes that were synthesized for single color ISH were used in fluorescent *in situ* hybridization (FISH). The same procedure for single chromagenic ISH was followed until after the RNAse treatment steps, with the exception of combining the two 500 μl of the diluted probes during the hybridization step. Following the second 0.2X SSC wash after RNAse treatment, embryos were washed twice for 15 minutes in PTw, then washed in 2% H_2O_2 in PTw for 60 minutes. Embryos were then washed twice in Tris-buffered saline with Tween 20 (TBST) for 15 minutes. The last wash was then replaced with 500 μl of 2% BMB in MAB for 5 minutes. Antibody incubation was done with 500 μl of a 1:1000 dilution of antibody conjugated to horseradish peroxidase in 2% BMB in MAB for 8-15 hours. Antibodies were washed out with 5 washes of TBST that lasted at least 1 hour each.

Fluophore Deposition

Fluophore was deposited by incubating embryos in 1 ml of an empirically
determined optimal dilution in PTw (Cy3 1:25, FITC 1:200) for 20 minutes. Hydrogen
peroxide was added to a final concentration of 0.3% and incubation continued for another
40 minutes. For the second deposition, the FISH procedure was repeated starting with the
2% H_2O_2 step. Following the final deposition, embryos were washed with TBST until
background was removed. Cleared whole mount images were created using the same
clearing procedure, microscope, camera, and software as above, with the exception that
fluorescent lights and fluorescein and rhodamine filters were used.

Cryosectioning

FISH embryos were incubated in 1.6 M sucrose in PBS at 4°C for several hours to
prepare for cyrosectioning. Embryos were then embedded in TBS medium (Triangle
Biosciences frozen sectioning medium) and frozen at -40 to -20°C on the freezing plate
of a Minotome cryostat (Triangle Biosciences) for at least 15 minutes. Transverse
sections were taken from tail to head and adhered to gelatin-coated slides. Coverslips
were mounted to slides with Vectashield Hardset (Vector Laboratories), and sections
were imaged using a Zeiss LSM 510 microscope. The Argon/2 laser was used to excite
fluorescein, and the HeNe543 laser was used to excite Cy3. The system was configured
so that FITC and Cy3 were detected on different channels, thereby eliminating bleed-
through of signal.

Immunohistochemistry

Embryos for immunohistochemistry were anesthetized, fixed in Dent's fixative (20% DMSO and 80% methanol, Dent *et al.,* 1989) for 2 hours at RT, and then moved to 4°C for an additional 8-15 hours. Embryos were then transferred to 100% methanol in 5 ml glass vials and stored at -20°C.

Expression of HNK-1 was identified by whole mount immunohistochemistry. Anti-HNK-1 monoclonal mouse IgM antibody (Sigma) was used with a goat anti-mouse IgG conjugated to alkaline phosphatase (Sigma) as the secondary antibody. Standard protocol was used for IHC using an alkaline phosphatase-catalyzed color reaction (Sive *et al.,* 2000), with the exception that embryos were initially fixed in Dent's fixative (Dent *et al.*, 1989). Embryos were rehydrated into PBS by successive 10 minute washes in 100% ethanol, 75% ethanol/25% H_2O, 50% ethanol/50% PBS, 25% ethanol/75% PBS, and 100% PBS; then incubated for 15 minutes in PBT (1X PBS, 0.1% Triton-X, 2 mg/ml Bovine Serum Albumin (Fisher)). Embryos were treated for 1 hour in 500 µl of a blocking solution consisting of 10% v/v goat serum in PBT. Blocking solution was replaced with 500 µl of primary antibody solution, in which HNK-1 antibody was diluted 1:10 in PBT. Embryos were incubated in antibody solutions for 8-15 hours at 4°C. Antibodies were washed out with 5 washes in PBT of at least 1 hour each. Embryos were incubated in a 1:2000 dilution of the secondary antibody for 8-15 hours. Secondary antibodies were washed out with 5 washes in PBT of at least 1 hour each. The color reaction was conducted as in alkaline phosphatase-catalyzed *in situ* color reactions, with the substitution of Triton-X-100 in place of Tween 20 in the AP buffer. IHC color reactions ranged from 15 minutes to 1 hour. Once sufficient signal had developed,

embryos were fixed in 1X MEMFA, stored in PBS, and analyzed in the same way that *in situ* processed embryos were.
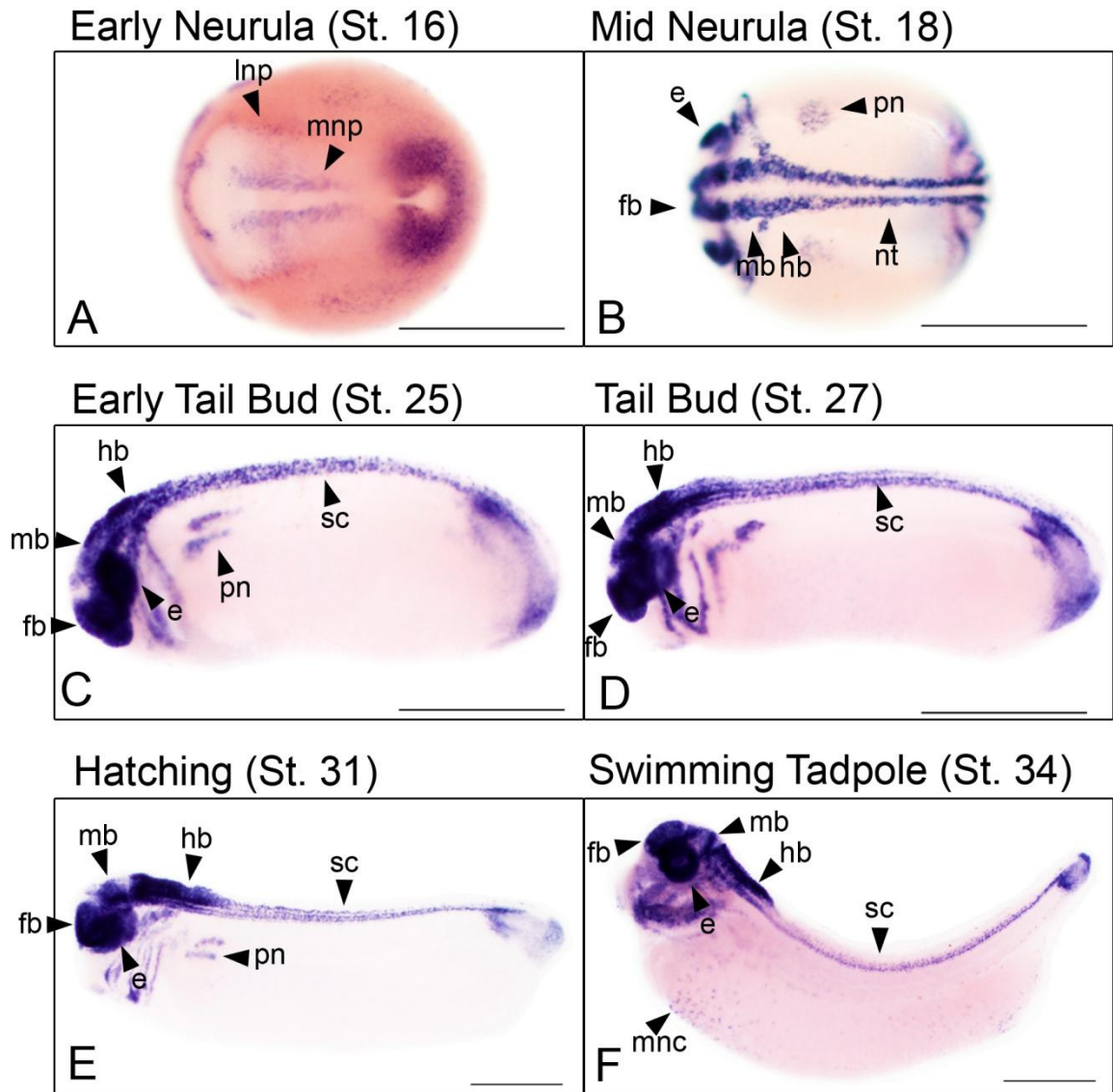
Results

Figure 1. Whole mount analysis of *X-Delta-1* expression from early neurula stage through swimming tadpole stage using *in situ* hybridization.

Figure 1. Whole mount analysis of *X-Delta-1* expression from early neurula stage through swimming tadpole stage using *in situ* hybridization. Embryos were cleared in BB:BA and photographed at (A) early neurula stage, (B) mid neurula stage, (C) early tail bud stage, (D) tail bud stage, (E) hatching stage, and (F) swimming tadpole stage. Arrowheads indicate regions of expression. Abbreviations: e, eye; fb, forebrain; hb, hindbrain; lnp, lateral neural plate; mb, midbrain; mnc, migratory neural crest; mnp, medial neural plate; nt, neural tube; pn, pronephros; sc, spinal cord. Scale bars represent 1 mm.
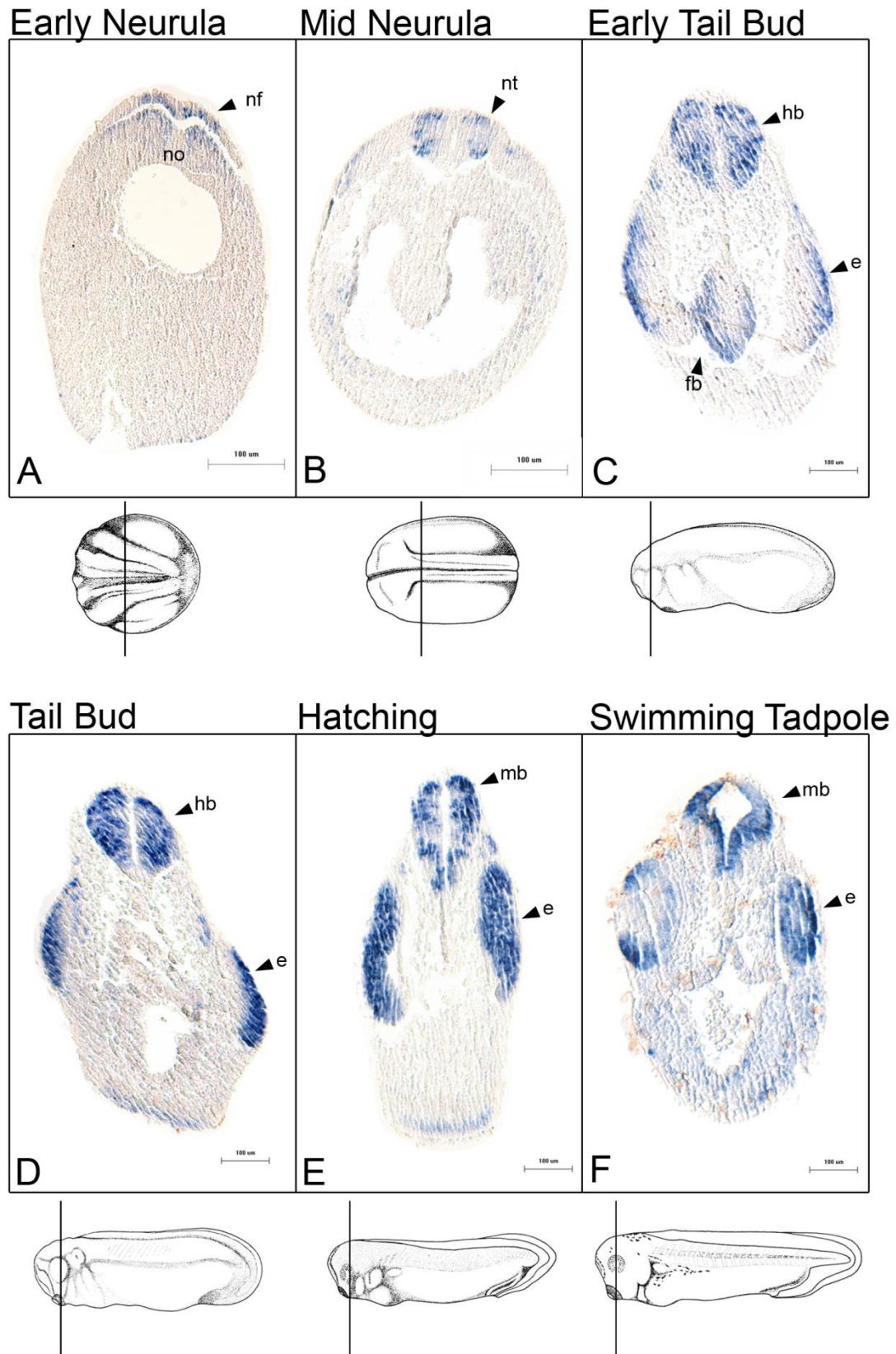
Figure 2. Histological analysis of *X-Delta-1* expression from early neurula stage through swimming tadpole stage using *in situ* hybridization.

Figure 2. Histological analysis of *X-Delta-1* expression from early neurula stage through swimming tadpole stage using *in situ* hybridization. Transverse 10 μm sections were taken from embryos at (A) early neurula stage, (B) mid neurula stage, (C) early tail bud stage, (D) tail bud stage, (E) hatching stage, and (F) swimming tadpole stage. Whole-embryo drawings (Neiuwkoop and Faber, 1994) indicate the positions of transverse sections on the anterior-posterior axis. Arrowheads indicate regions of expression and text indicates anatomical structures. Abbreviations: e, eye; fb, forebrain; hb, hindbrain; mb, midbrain; no, notochord; nf, neural fold; nt, neural tube. Scale bars represent 100 μm.

Figure 3. Whole mount analysis of *X-Notch ICD* expression from early neurula stage through swimming tadpole stage using *in situ* hybridization.

Figure 3. Whole mount analysis of *X-Notch ICD* expression from early neurula stage through swimming tadpole stage using *in situ* hybridization. Embryos were cleared in BB:BA and photographed at (A) early neurula stage, (B) mid neurula stage, (C) late neurula stage, (D) early tail bud stage, (E) hatching stage, and (F) swimming tadpole stage. Arrowheads indicate regions of expression. Abbreviations: e, eye; fb, forebrain; hb, hindbrain; mb, midbrain; nf, neural fold; nt, neural tube; sc, spinal cord. Scale bars represent 1 mm.
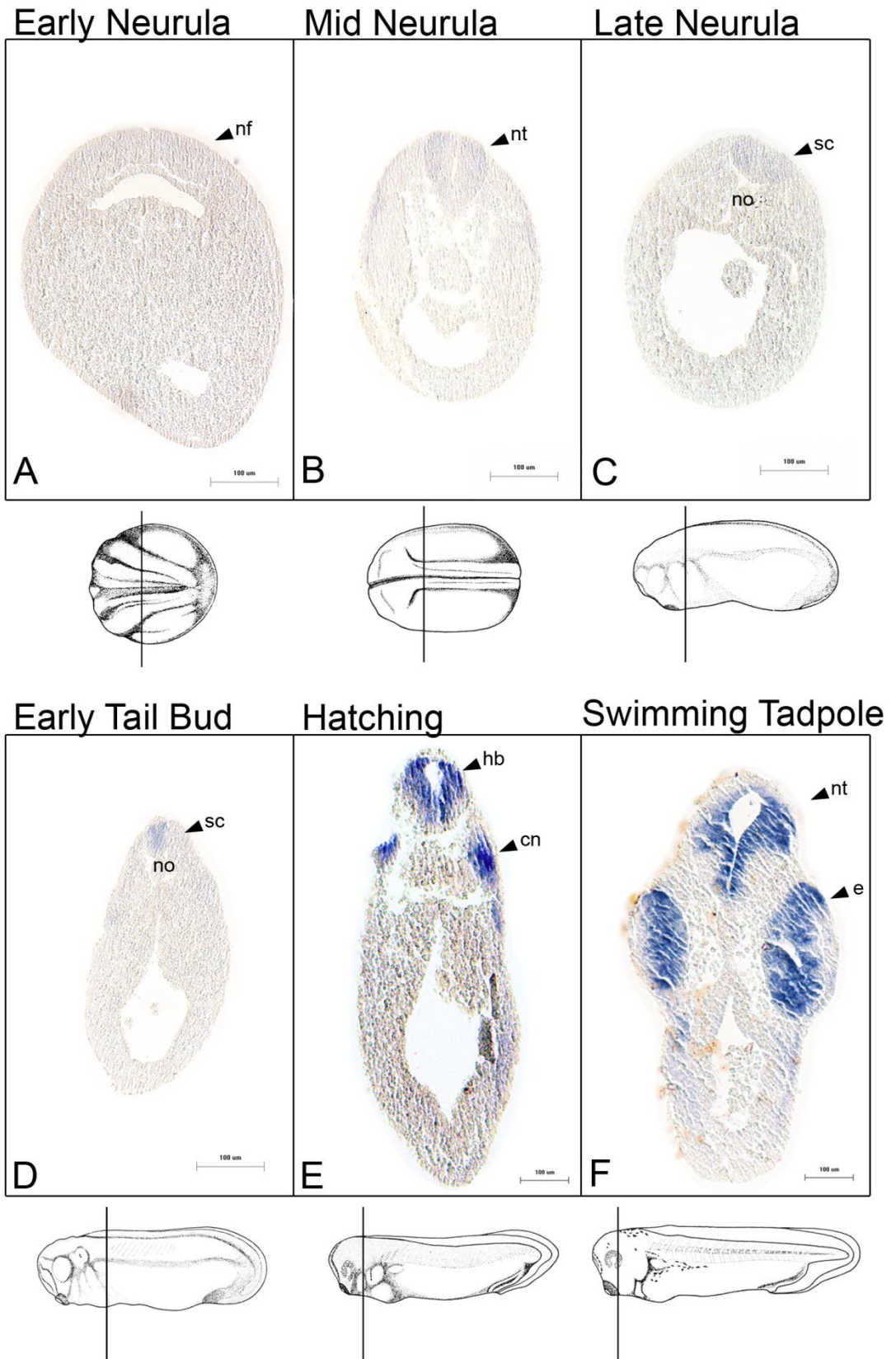
Early Neurula **Mid Neurula** **Late Neurula**

Early Tail Bud **Hatching** **Swimming Tadpole**

Figure 4. Histological analysis of *X-Notch ICD* expression from early neurula stage through swimming tadpole stage using *in situ* hybridization.

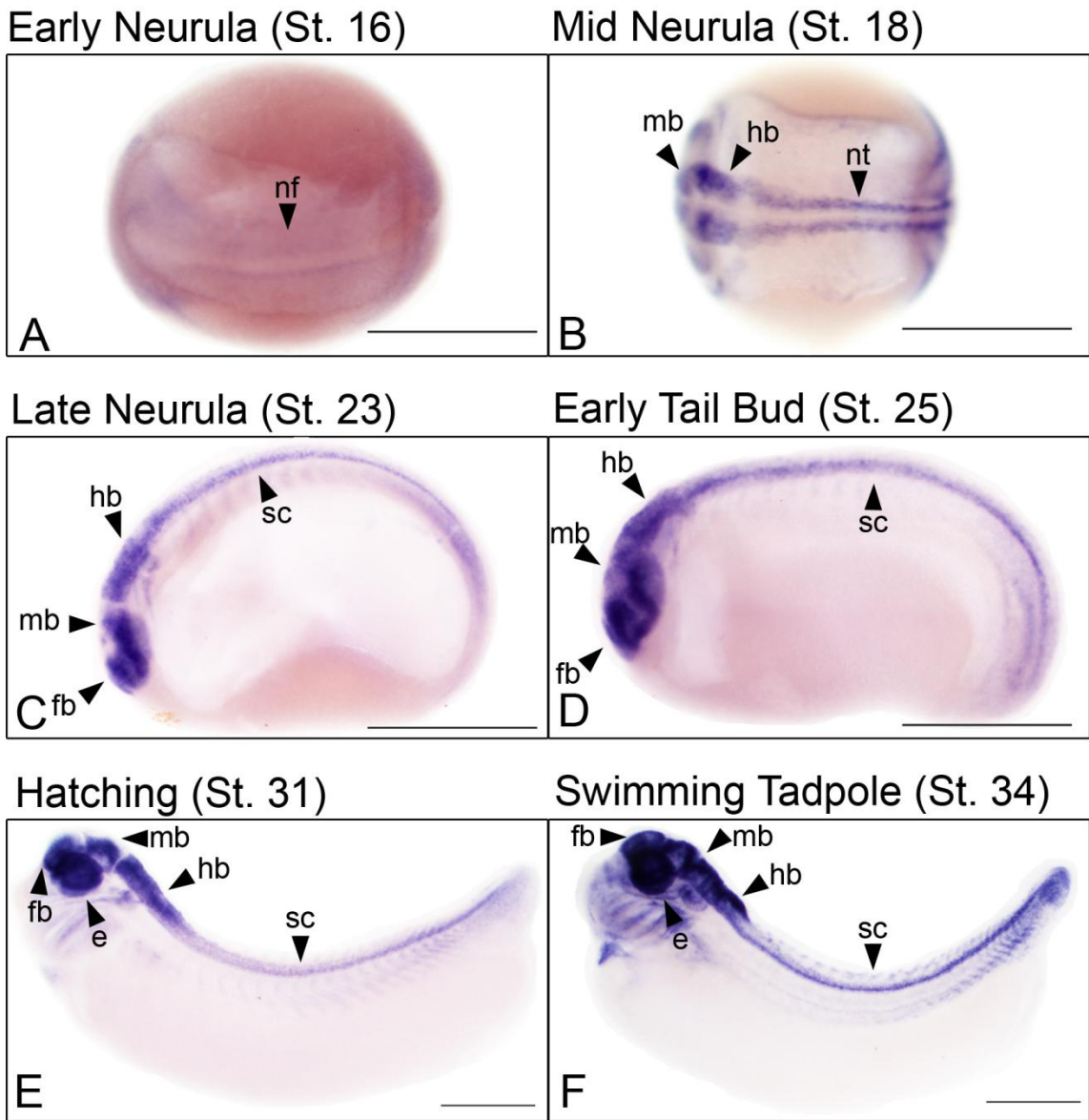**Figure 4.** Histological analysis of *X-Notch ICD* expression from early neurula stage through swimming tadpole stage using *in situ* hybridization. Transverse 10 μm sections were taken from embryos at (A) early neurula stage, (B) mid neurula stage, (C) late neurula stage, (D) early tail bud stage, (E) hatching stage, and (F) swimming tadpole stage. Whole-embryo drawings (Neiuwkoop and Faber, 1994) indicate positions of transverse section on the anterior-posterior axis. Arrowheads indicate regions of expression and text indicates anatomical structures. Abbreviations: cn, cranial nerve; e, eye; fb, forebrain; hb, hindbrain; mb, midbrain; no, notochord; nf, neural fold; nt, neural tube; sc, spinal cord. Scale bars represent 100 μm.
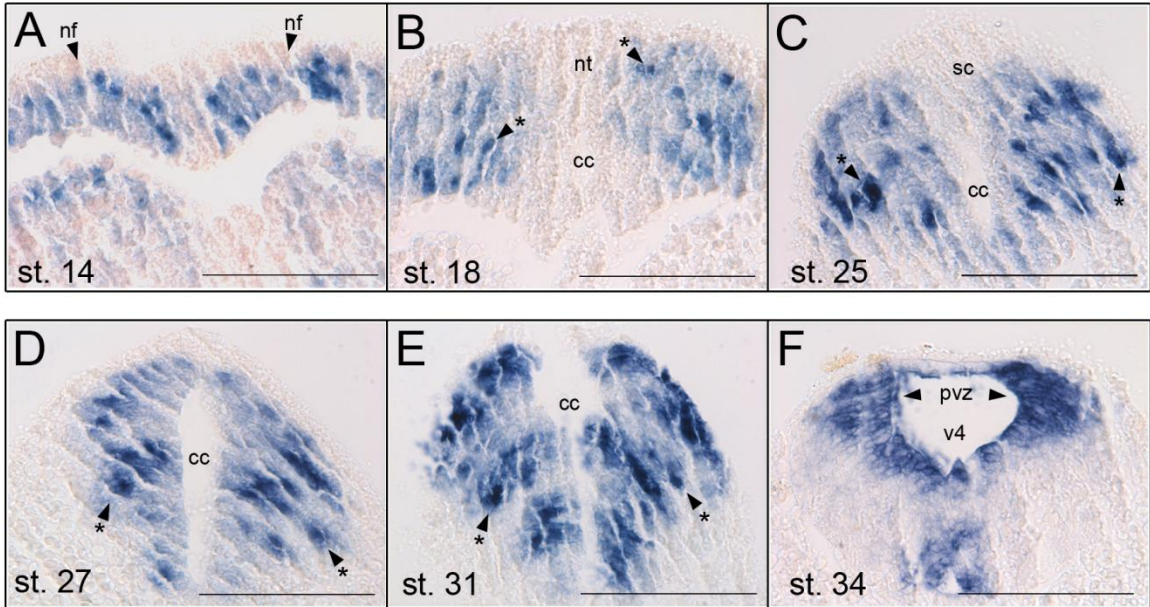
X-Delta-1 Histology Detail

X-Notch ICD Histology Detail
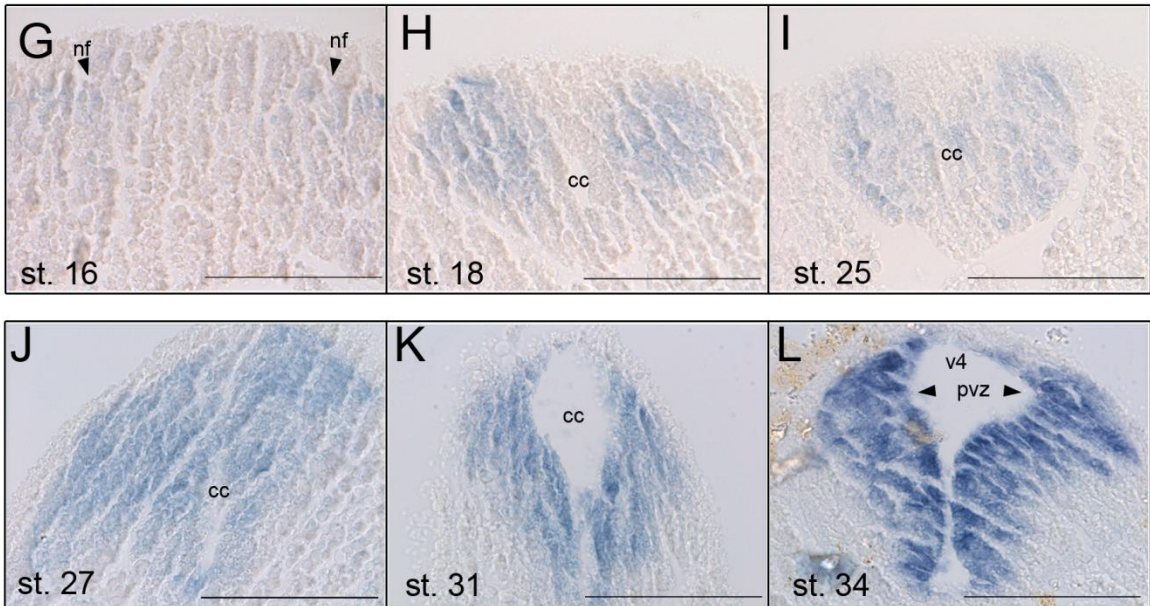
Figure 5. High-magnification histological analysis of *X-Delta-1* and *X-Notch ICD* expression.

Figure 5. High-magnification histological analysis of *X-Delta-1* and *X-Notch ICD* expression. Images of 10 μm transverse sections were captured at 400X magnification. Sections (A-F) are magnified versions of X-Delta-1 assayed embryos depicted in Figure 2, at similar positions on the anterior-posterior axis; sections (G-L) are magnified versions of X-Notch ICD assayed embryos depicted in Figure 4, at similar positions on the anterior-posterior axis. Asterisks indicate examples of dense, isolated points of X-Delta-1 expression, arrowheads indicate regions of expression, and text indicates anatomical structures. Abbreviations: cc, central canal; nf, neural fold; pvz, periventricular zone; v4, fourth ventricle of the brain. Scale bars represent 100 μm.

Figure 6. Whole mount analysis of *xNBT*, *xGAT1*, and *xVGlut1* expression in non-injected, vehicle-injected, X-Notch ICD-injected, and xSu(H) DBM-injected embryos using whole mount *in situ* hybridization.

	Gross Defects	NTD's	+ xNBT	- xNBT	+ xVGlut1	- xVGlut1	+ xGAT1	- xGAT1
X-Notch-ICD	130/232	50/230	0/18	2/18	0/17	4/17	1/18	7/18
xSu(H)-DBM	155/241	18/241	16/60	1/60	17/59	2/59	1/10	0/10
GFP	0/45	0/45	0/15	0/15	0/15	0/15	0/15	0/15

Table 1. Summary of observed phenotypes in embryos injected with X-Notch ICD, xSu(H) DBM, of GFP.
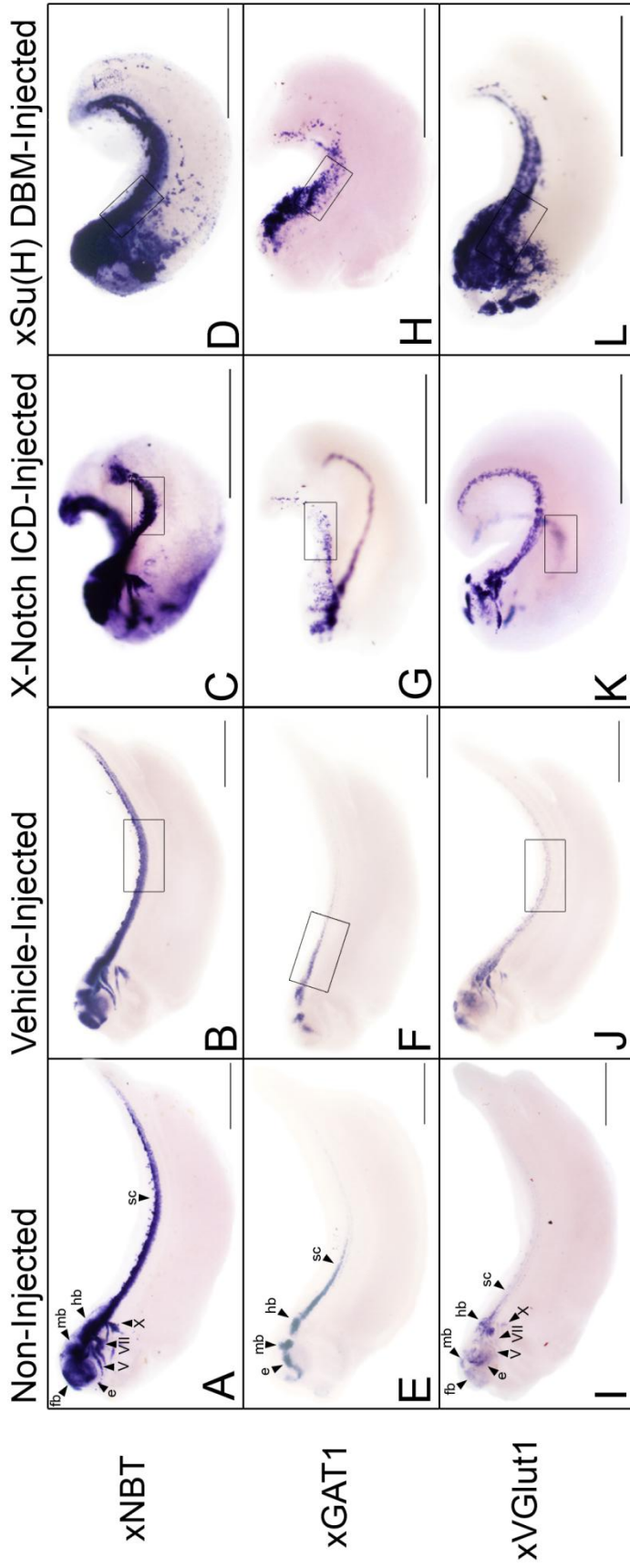
47

Figure 6. Whole mount analysis of *xNBT*, *xGAT1*, and *xVGlut1* expression in non-injected, vehicle-injected, X-Notch ICD-injected, and xSu(H) DBM-injected embryos using whole mount *in situ* hybridization. Embryos were cleared in BB:BA and photographed in bright field. Embryos (A, E, and I) are non-injected controls, (B, F, and J) are vehicle-injected controls injected with 4.6nl water with 0.5ng GFP mRNA, (C, G, and K) are embryos injected with 4.6nl water with 1.5ng X-Notch ICD mRNA and 0.5ng GFP mRNA, (D, H, and L) are embryos injected with 4.6 nl water with 1.5ng xSu(H) DBM mRNA and 0.5ng GFP mRNA. Embryos (A-D) were assayed for *xNBT*, (E-H) were assayed for *xGAT1*, (I-L) were assayed for *xVGlut1*. In images (B-D, G-H, J, and L) the injected side of embryo is in the plane of focus, in (H) the un-injected side of the embryo is in the plane of focus. Arrowheads indicate regions of expression in non-injected controls. Abbreviations: e, eye; fb, forebrain; hb, hindbrain; mb, midbrain; sc, spinal cord; V, cranial nerve V; VII, cranial nerve VII; X, cranial nerve X. Inset boxes represent areas that are magnified in Figure 5. Scale bars represent 1 mm.

Table 1. Summary of observed phenotypes in embryos injected with X-Notch ICD, xSu(H) DBM, or GFP. "Gross Defects" represents embryos that had abnormal gross morphologies; "NTD's" represents embryos that had neural tube closure defects; "+ xNBT", "+ xVGlut1", and "+ xGAT1" represent embryos that showed increased expression of respective marker; "- xNBT", "- xVGlut1", and "- xGAT1" represent embryos that showed decreased expression of respective marker. Numbers shown as observed phenotypes / total.
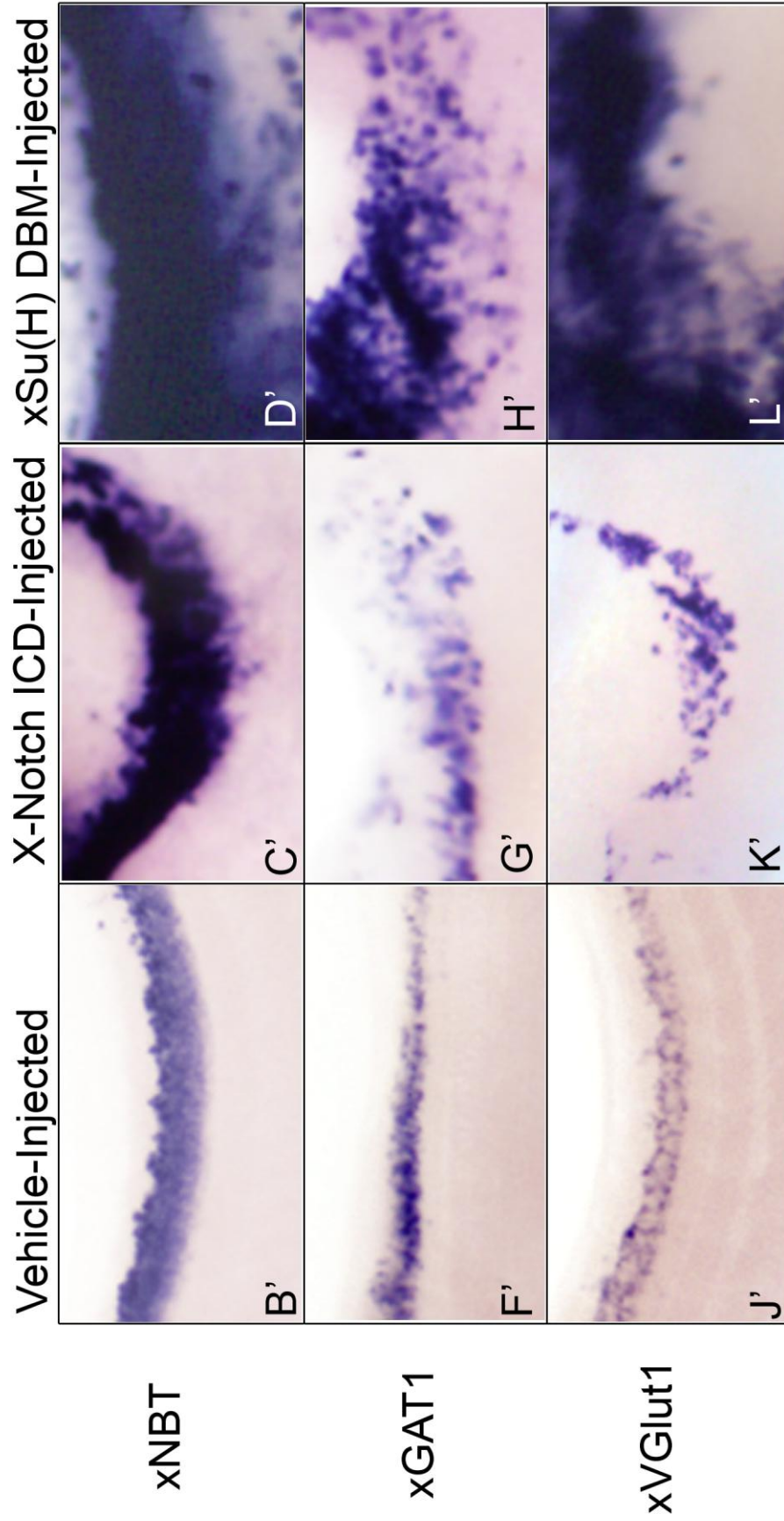
Figure 7. Details of whole mount analysis of *xNBT*, *xGAT1*, and *xVGlut1* expression in non-injected, vehicle-injected, X-Notch ICD-injected, and xSu(H) DBM-injected embryos using whole mount *in situ* hybridization shown in **Figure 6.**

Figure 7. Details of whole mount analysis of *xNBT*, *xGAT1*, and *xVGlut1* expression in non-injected, vehicle-injected, X-Notch ICD-injected, and xSu(H) DBM-injected embryos using whole mount *in situ* hybridization shown in Figure 6. Area of image corresponds to area enclosed within the boxes of Figure 6. Magnified images (B'-D', G', J', and L') were taken from original images from Figure 6, (H') is a magnified image taken from image in which injected side of the embryo is in the plane of focus.
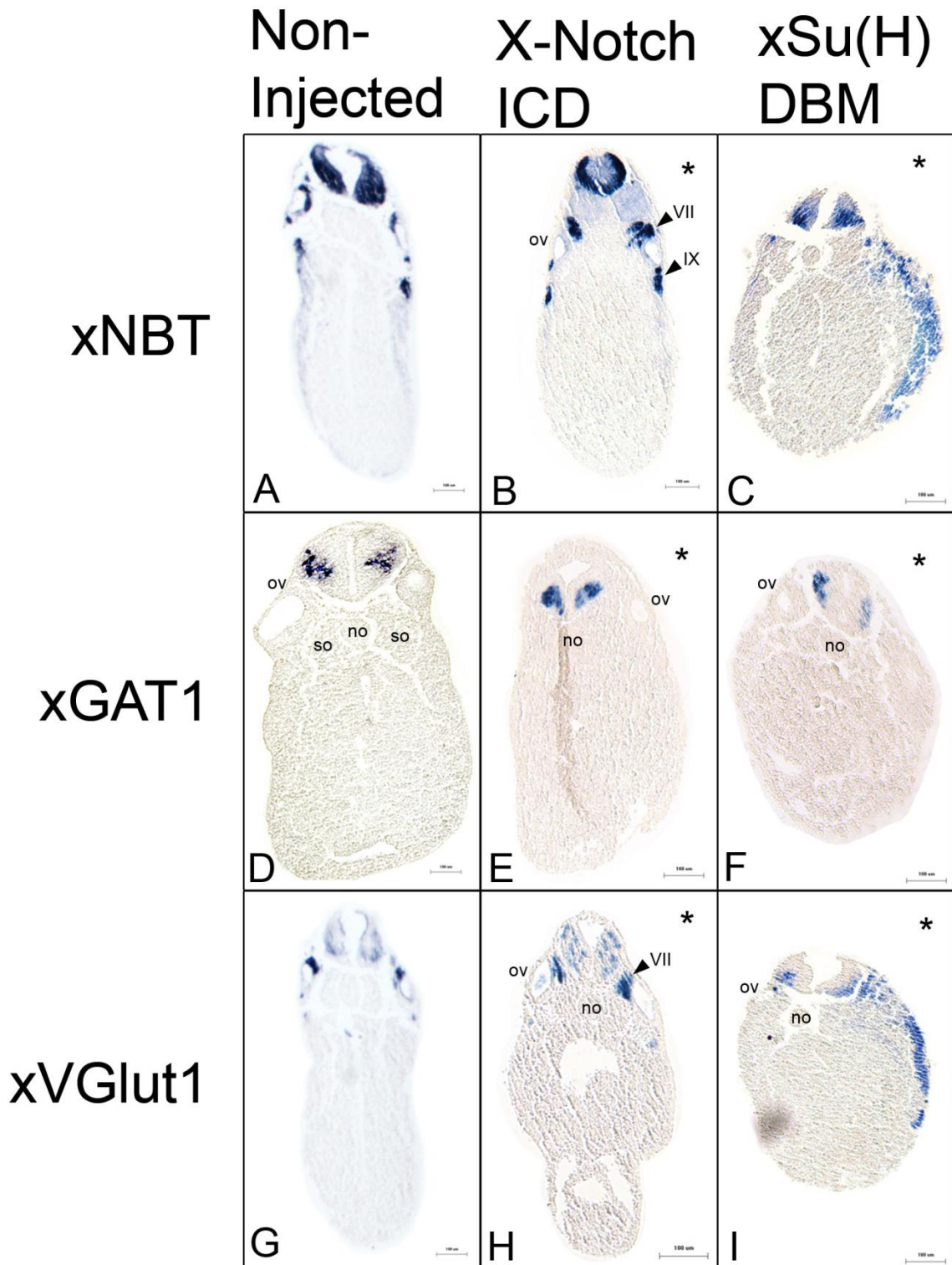
Figure 8. Histological analysis of *xNBT*, *xGAT1*, and *xVGlut1* expression in non-injected, X-Notch ICD-injected, and xSu(H) DBM-injected embryos using whole mount *in situ* hybridization.
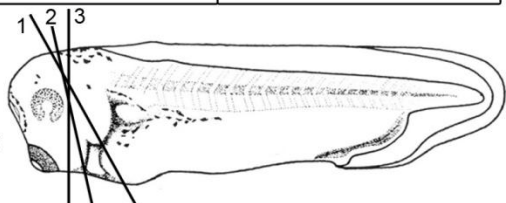
Figure 8. Histological analysis of *xNBT*, *xGAT1*, and *xVGlut1* expression in non-injected, X-Notch ICD-injected, and xSu(H) DBM-injected embryos using whole mount *in situ* hybridization at swimming tadpole stages. 10 μm transverse sections were photographed using bright field photography at 40x magnification. Images (A, D, and G) are non-injected controls, (B, E, and H) are injected with 4.6nl water with 1.5ng X-Notch ICD mRNA and 0.5ng GFP mRNA, (C, F, and I) are injected with 4.6nl 1.5ng xSu(H) DBM mRNA and 0.5ng GFP mRNA. Embryos (A-C) were assayed for *xNBT*, (D-F) were assayed for *xGAT1,* and (G-I) were assayed for *xVGlut1*. Transverse section (H) was taken through plane 1, (A, B, and G) were taken through plane 2; (C-F, and I) were taken through plane 3. Arrowheads indicate regions of expression, text indicates anatomical features, and asterisks indicate the injected side of the embryo. Abbreviations: no, notochord; ov, otic vesicle; so, somite; VII, cranial nerve VII; IX, cranial nerve IX. Scale bars represent 100 μm.

Vehicle-Injected

xSu(H) DBM-Injected

xNBT
Mid Neurula
(st. 21)

Uninjected Side

xSu(H) DBM-Injected Side

xVGlut1
Hatching
(st. 30)
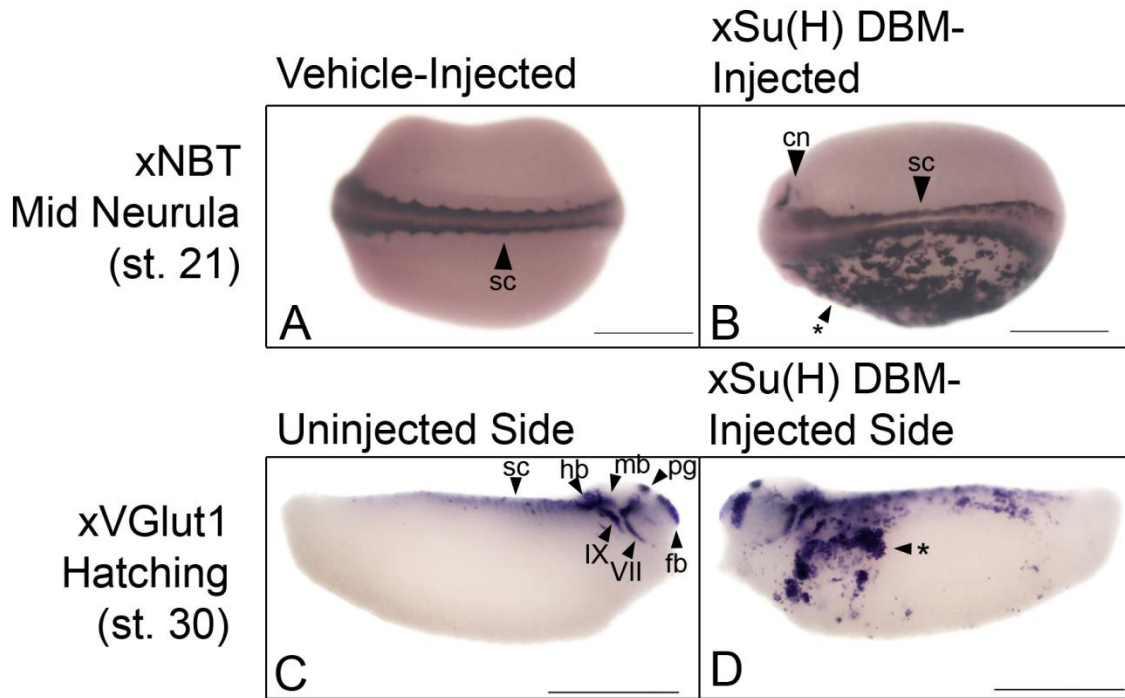
Antisense Probe	# Showing Ectopic Expression
xNBT (st. 21)	9/12
xNBT (st. 35)	16/60
xVGlut1	17/59
xGAT1	0/60
xTH	0/20
xChat	0/20
xSert	0/18
xSlug	0/34

Table 2. Summary of observed ectopic expression in embryos injected xSu(H) DBM.

40X   400X

xNBT

xVGlut1

Figure 9. Whole mount and histological analysis of ectopic expression of *xNBT* and *xVGlut1* in xSu(H) DBM-injected embryos using *in situ* hybridization.
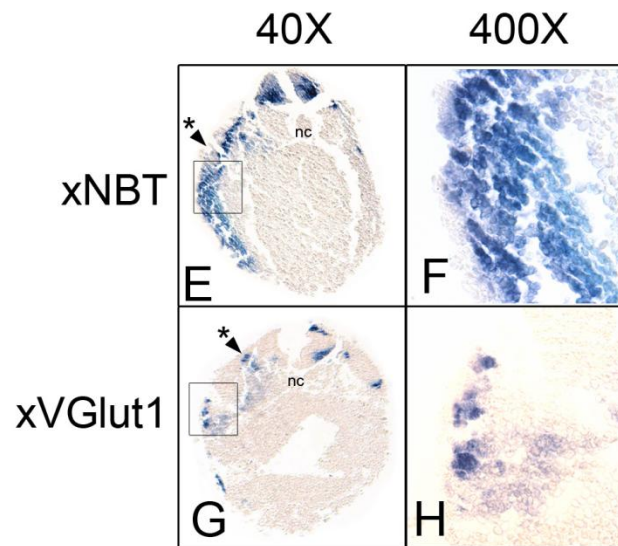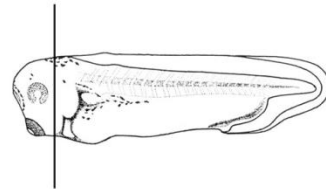
Figure 9. Whole mount and histological analysis of ectopic expression of *xNBT* and *xVGlut1* in xSu(H) DBM-injected embryos using *in situ* hybridization. Embryo (A) was injected with 4.6nl water with 0.5ng GFP mRNA, and (B-H) were injected with 4.6nl water with 1.5ng xSu(H) DBM mRNA and 0.5ng GFP mRNA. Images (A-D) are bright field photographs of embryos in 1x PBS, and (E-H) are 10 μm transverse sections of swimming tadpole stage embryos showing ectopic expression. Mid neurula stage embryos (A and B) were assayed for *xNBT*, and a hatching stage embryo (C and D) was assayed for *xVGlut1*. Image (A) is the dorsal view of a vehicle-injected control embryo, (B) is the dorsal view of an embryo injected with xSu(H)-DBM mRNA, (C) is the uninjected side of an injected embryo, (D) is the injected side of the embryo in (C). Images (E and G) are transverse sections captured at 40X magnification, and images (F and H) are transverse sections captured at 400X magnification, corresponding to the respective inset boxes in (E and G). Whole-embryo drawing (Neiuwkoop and Faber, 1994) indicates position of the transverse sections on the anterior-posterior axis. The embryo in (E and F) was assayed for *xNBT*, (G and H) was assayed for *xVGlut1*. Arrowheads indicate regions of expression in vehicle-injected embryo (A) or the uninjected side of injected embryo (B and C). Asterisks indicate ectopic expression on the injected side of the embryo in (B, D, E, and G), text indicates anatomical structures in (E and G). Abbreviations: cn, cranial nerve; fb, forebrain; hb, hindbrain; mb, midbrain; nc, notochord; pg, pineal gland; sc, spinal cord; VII, cranial nerve VII; IX, cranial nerve IX. Scale bars in (A-D) represent 1 mm.

Table 2. Summary of observed ectopic expression in embryos injected xSu(H) DBM. Embryos were injected with 4.6nl water with 1.5ng xSu(H) DBM mRNA and 0.5ng GFP mRNA and assayed for various phenotype markers at swimming tadpole stages, unless otherwise indicated. Ectopic expression refers to expression that is outside of the regions in which expression is normally observed in non-injected or vehicle-injected controls. Numbers shown as embryos showing ectopic expression / total.

Figure 10.1 Whole mount analysis of *xTH*, *xSert*, and *xChat* expression in non-injected, vehicle-injected, and xSu(H) DBM-injected embryos using *in situ* hybridization.

Figure 10.2 Histological analysis of *xNBT* and *xVGlut1* expression in non-injected and xSu(H) DBM-injected embryos using double fluorescent *in situ* hybridization.
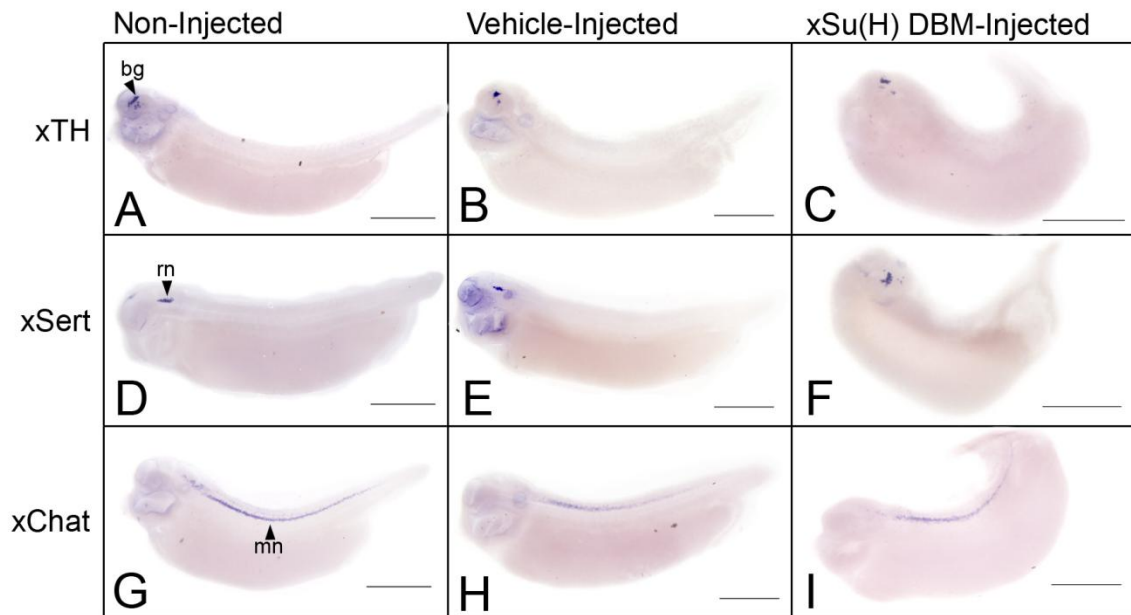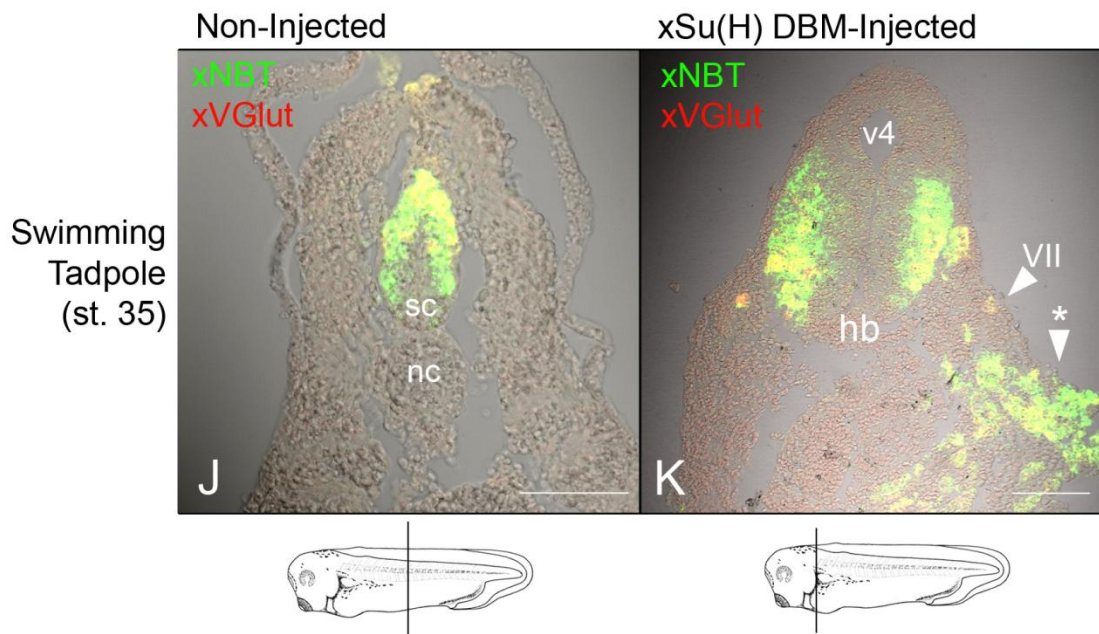
Figure 10.1 Whole mount analysis of *xTH*, *xSert*, and *xChat* expression in non-injected, vehicle-injected, and xSu(H) DBM-injected embryos using whole mount *in situ* hybridization. Embryos were cleared in BB:BA and photographed in bright field at swimming tadpole stage. Embryos (A, D, and G) are non-injected controls, (B, E, and H) are vehicle-injected controls injected with 4.6nl water with 0.5ng GFP mRNA; (C, F, and I) were injected with 4.6 nl water with 1.5ng xSu(H) DBM mRNA and 0.5ng GFP mRNA. Embryos (A-C) were assayed for *xTH*, (D-F) were assayed for *xSert*, and (G-I) were assayed for *xChat*. Arrowheads indicate regions of expression in non-injected controls. Abbreviations: bg, basal ganglia; mn, motor neurons; rn, raphe nucleus. Scale bars represent 1 mm.

Figure 10.2 Histological analysis of *xNBT* and *xVGlut1* expression in non-injected and xSu(H) DBM-injected embryos using double fluorescent *in situ* hybridization. Sections (J and K) are swimming tadpole stage embryos imaged via multi-channel confocal microscopy. Embryo (J) is a non-injected control, and (K) was injected with 4.6nl water with 1.5ng xSu(H) DBM mRNA and 0.5 ng GFP mRNA. Expression of *xNBT* was labeled with FITC and appears green, *xVGlut1* was labeled with Cy3 and appears red, and areas of overlapping expression appear yellow. Whole-embryo drawings (Neiuwkoop and Faber, 1994) indicate positions of the transverse sections on the anterior-posterior axis. Arrowheads indicate regions of expression, text indicates anatomical structures, and asterisks indicate ectopic expression on the injected side of the embryo. Abbreviations: hb, hindbrain; nc, notochord; sc, spinal cord; VII, cranial nerve VII; v4, fourth ventricle of the brain. Scale bars represent 100 μm.

Figure 11.1 Whole mount analysis of HNK-1 protein expression in embryos injected with xSu(H) DBM using whole mount immunohistochemistry.

Figure 11.2 Detail images of selected regions from **Figure 11.1**.

Treatment	# Showing Ectopic Expression
Non-Injected	0/60
Vehicle-Injected	0/4
DBM-Injected	44/72

Table 3. Summary of ectopic HNK-1 protein expression in non-injected, vehicle-injected, and xSu(H) DBM-injected embryos using immunohistochemistry.

57

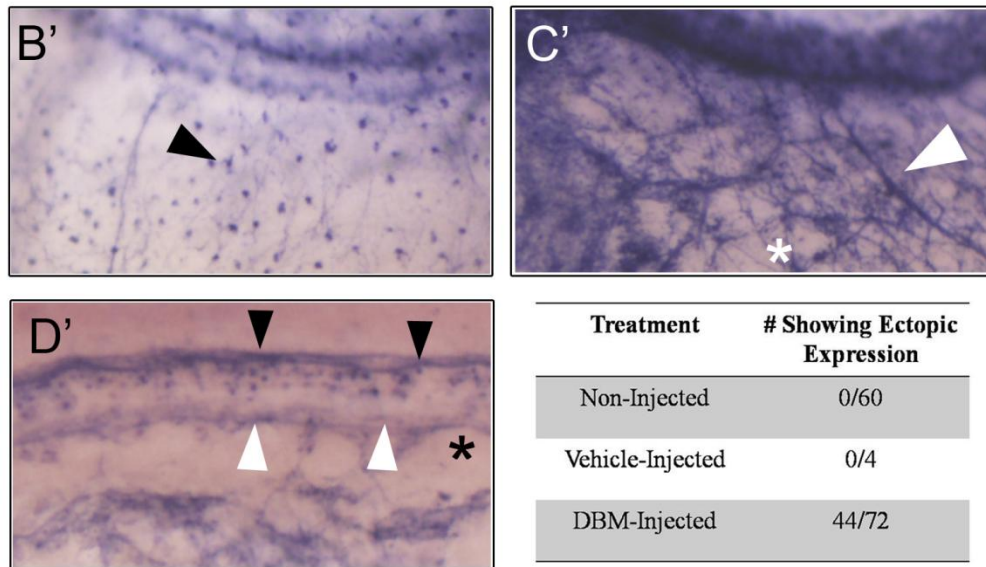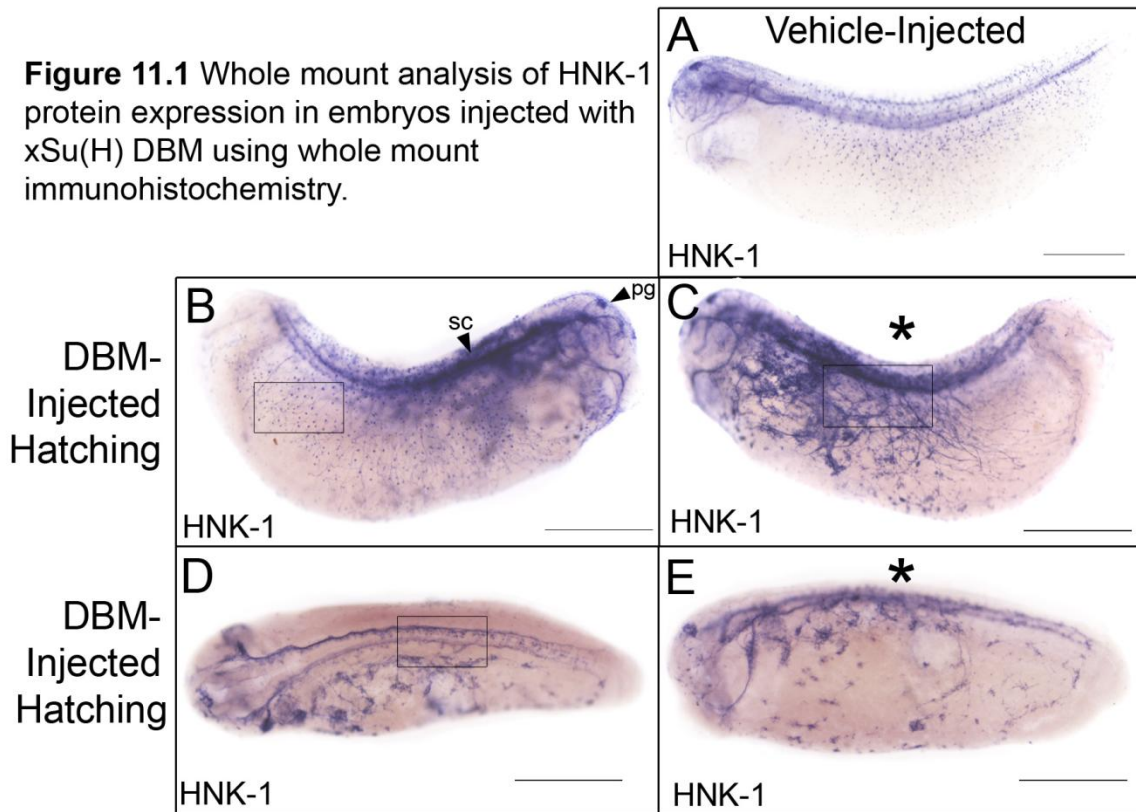**Figure 11.1** Whole mount analysis of HNK-1 protein expression in embryos injected with xSu(H) DBM using whole mount immunohistochemistry. Embryos were cleared in BB:BA and bright field photographs were taken at hatching stage. Embryo (A) is a vehicle-injected control injected with 4.6nl water with 0.5ng GFP mRNA, (B-E) were injected with 4.6nl water with 1.5ng xSu(H)-DBM mRNA and 0.5ng GFP mRNA. Image (B) is the uninjected side of an embryo, (C and E) are injected sides of embryos, and (D) is the dorsal view of an embryo. Image (C) is the opposite view of (B), and (E) is the lateral view of (D). Arrowheads indicate regions of expression on the uninjected side of the embryo and asterisks indicate ectopic expression on the injected side of the embryo. Abbreviations: pg, pineal gland; sc, spinal cord. Inset boxes in (B, C, and E) represent magnified areas shown in Figure 11.2, as B', C', and E'). Scale bars represent 1 mm.

Figure 11.2 Detail images of selected regions from Figure 11.1. (B') Detail of uninjected side of embryo, arrowhead indicates example of post-migratory neural crest. (C') Detail of injected side of embryo, asterisk indicates ectopic expression and arrowhead indicates apparent axon. (D') Detail of dorsal view of injected embryo showing both injected (bottom) and uninjected (top) sides. Black arrowheads indicate cell bodies on the uninjected side, white arrowheads mark the absence of similar cell bodies on the injected side.

Table 3. Summary of ectopic HNK-1 protein expression in non-injected, vehicle-injected, and xSu(H) DBM-injected embryos using immunohistochemistry. Vehicle-injected embryos were injected with 4.6nl water with 0.5ng GFP mRNA and xSu(H) DBM-injected embryos were injected with 4.6nl water with 1.5ng xSu(H)-DBM mRNA and 0.5ng GFP mRNA. Embryos were assayed from hatching stages to swimming tadpole stages. Numbers shown as embryos showing ectopic expression / total.

Figure 12.1 Whole mount analysis of *xVim* expression in xSu(H) DBM-injected embryos.

A hb Non-Injected
sc
V VII
ims
xVim

DBM-Injected Swimming Tadpole

B *xVim*

C *xVim*

DBM-Injected Swimming Tadpole

D *xVim*

E *xVim*
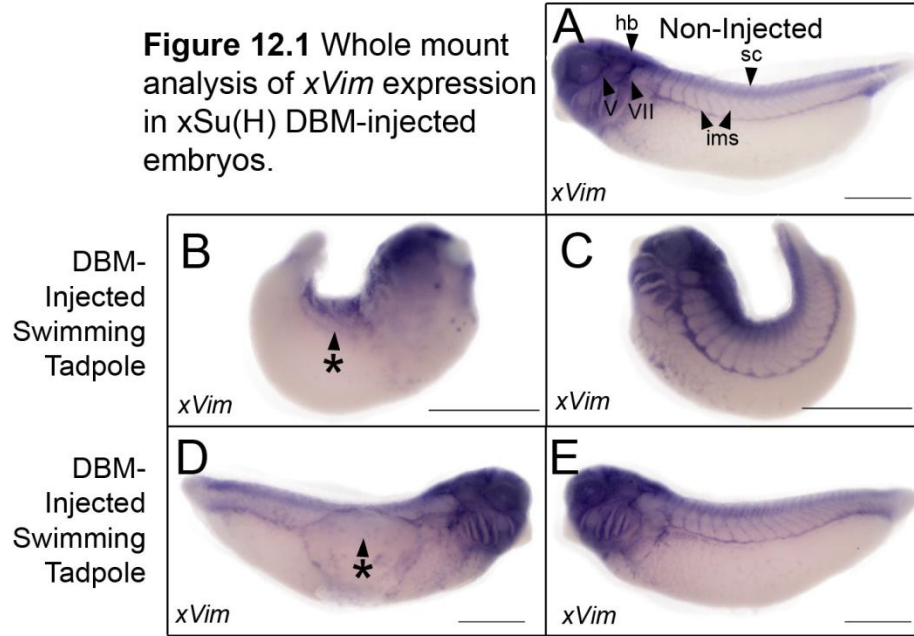
	No Change	Increased xVim	Decreased xVim
Su(H)-DBM Injected	8/23	0/23	12/23

Table 4. Summary of *xVim* expression in xSu(H) DBM-injected embryos using whole mount *in situ* hybridization at swimming tadpole stages.

Non-Injected — Su(H) DBM-Injected

xSlug
xVGlut
nc
sc
no
F

xSlug
xVGlut
*
sc
no
G

Early Tail Bud (st. 25)

Figure 12.2 Histological analysis of *xSlug* and *xVGlut1* expression in non-injected and xSu(H) DBM-injected embryos using double fluorescent *in situ* hybridization.

Figure 12.1 Whole mount analysis of *xVim* expression in xSu(H) DBM-injected embryos. Bright field photographs were taken of swimming tadpole stage embryos assayed for *xVim*, in 1x PBS. Embryo (A) is a non-injected control, (B-E) were injected with 4.6nl water with 1.5ng xSu(H)-DBM mRNA and 0.5ng GFP mRNA. Images (B and D) are the injected sides of embryos, (C and E) are uninjected sides of embryos and are the opposite of embryos (B and D), respectively. Arrowheads indicate regions of expression and asterisks indicate decreased expression on the injected side. Abbreviations: hb, hindbrain; ims, intermyotomal spaces; sc, spinal cord; V, cranial nerve V; VII, cranial nerve VII. Scale bars represent 1 mm.

Table 4. Summary of *xVim* expression in xSu(H) DBM-injected embryos using whole mount *in situ* hybridization at swimming tadpole stages. Embryos were injected with 4.6nl water with 1.5ng xSu(H) DBM mRNA. Numbers indicate the number of embryos out of the total that showed no change in *xVim* expression, increased *xVim* expression, or decreased *xVim* expression.
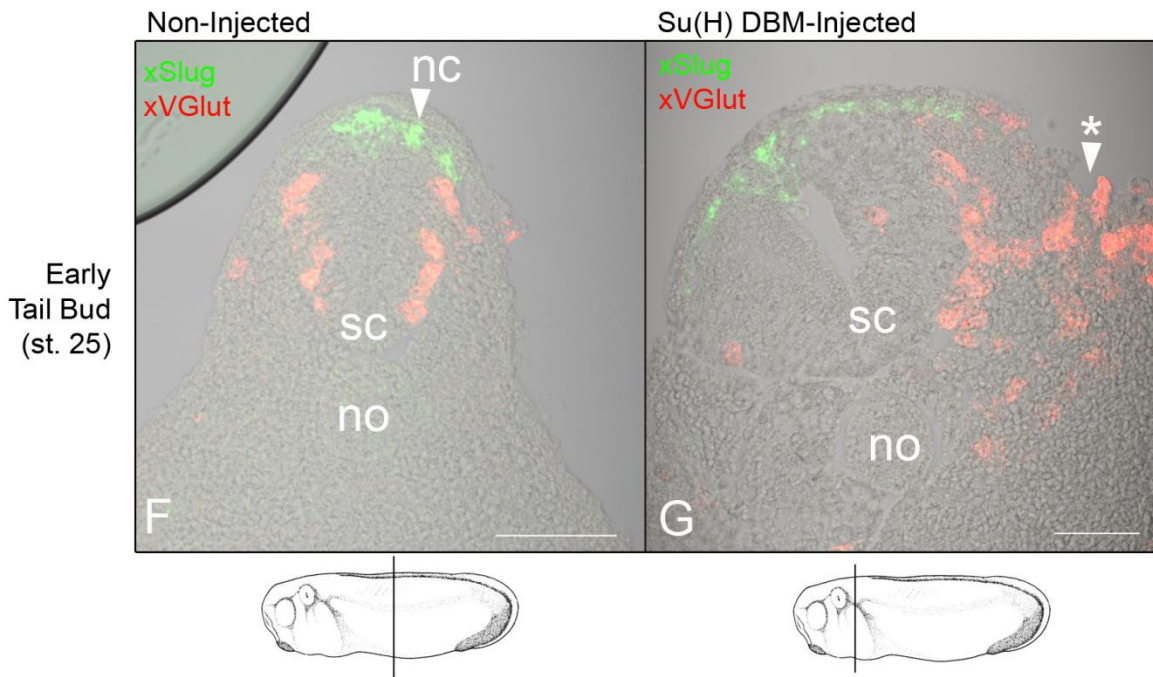
Figure 12.2 Histological analysis of *xSlug* and *xVGlut1* expression in non-injected and xSu(H) DBM-injected embryos using double fluorescent *in situ* hybridization. Sections (F and G) are from early tail bud stage embryos imaged via multi-channel confocal microscopy. Embryo (F) is a non-injected control, and (G) was injected with 4.6nl water with 1.5ng xSu(H) DBM mRNA and 0.5 ng GFP mRNA. Expression of *xSlug* was labeled with FITC and appears green, *xVGlut1* was labeled with Cy3 and appears red, and areas of overlapping expression appear yellow. Whole-embryo drawings (Neiuwkoop and Faber, 1994) indicate the position of the transverse sections on the anterior-posterior axis. Arrowheads indicate regions of expression, text indicates anatomical structures, and asterisks indicate ectopic expression on the injected side of the embryo. Abbreviations: hb, hindbrain; no, notochord; nc, neural crest; sc, spinal cord; VII, cranial nerve VII; v4, fourth ventricle of the brain. Scale bars represent 100 μm.
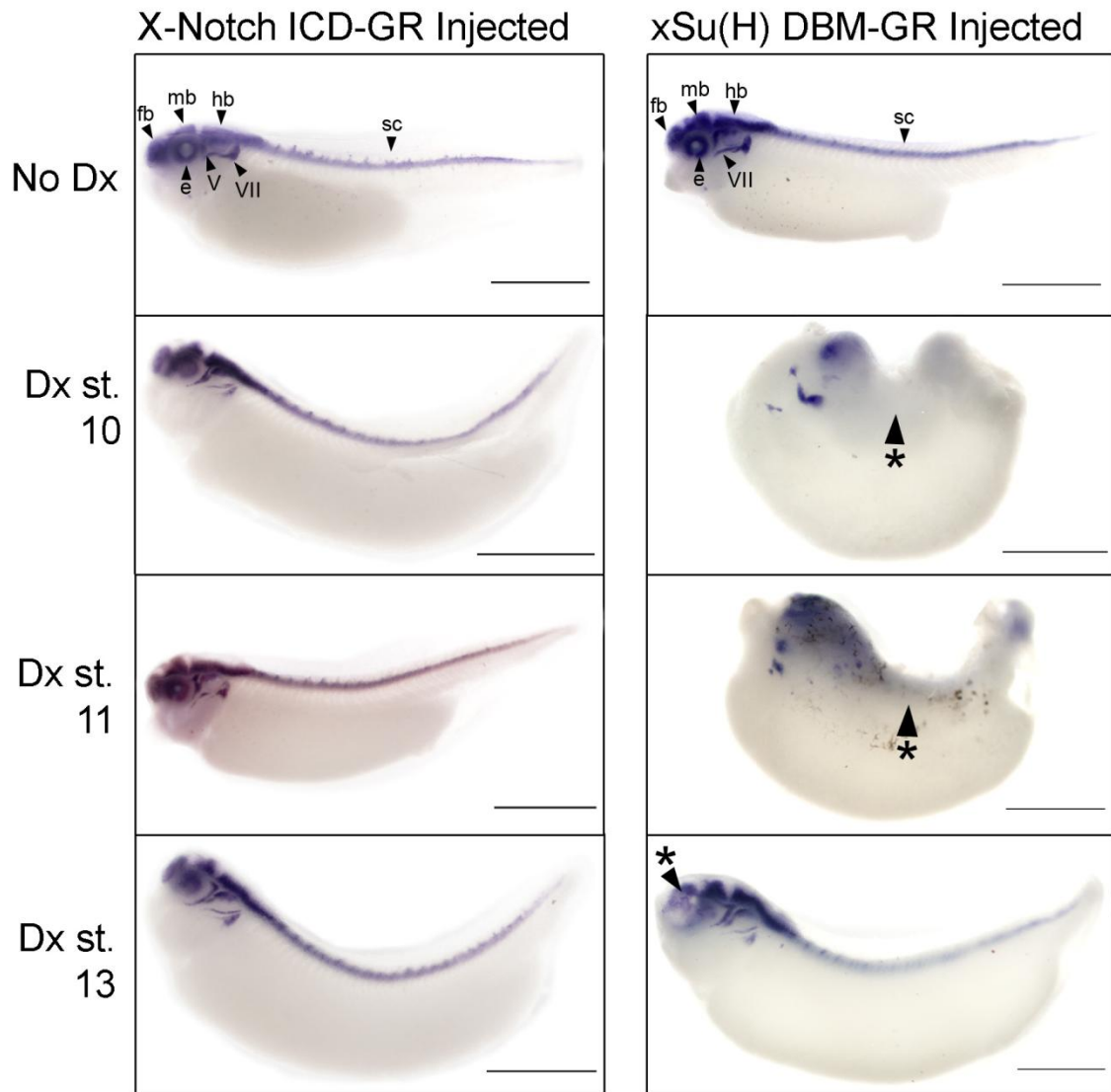
Figure 13. Whole mount analysis of *xNBT* expression in embryos injected with X-Notch ICD-GR or xSu(H) DBM-GR using *in situ* hybridization.

Figure 13. Whole mount analysis of *xNBT* expression in embryos injected with X-Notch ICD-GR or xSu(H) DBM-GR using *in situ* hybridization. Bright field photographs of embryos assayed for *xNBT* were taken in 1x PBS. Embryos (A-D) were injected with 4.6nl water with 1.5ng X-Notch ICD-GR and 0.5ng GFP mRNA, and (E-H) were injected with 4.6nl water with 1.5ng xSu(H) DBM-GR and 0.5ng GFP mRNA. Swimming tadpole stage control embryos (A and E) were not treated with dexamethasone, (B and F) were treated with dexamethasone prior to NF stage 10, (C and G) were treated with dexamethasone at NF stage 11, and (D and H) were treated with dexamethasone at NF stage 13. Arrowheads indicate regions of expression in control embryos and asterisks indicate regions of decreased expression in injected embryos. Abbreviations: e, eye; fb, forebrain; hb, hindbrain; mb, midbrain; sc, spinal cord; V, cranial nerve V; VII, cranial nerve VII. Scale bars represent 1 mm.

X-Delta-1 Expression

In order to determine if Notch signaling could be involved in neurotransmitter phenotype specification, we assayed for the expression of the ligand *X-Delta-1* and the receptor *X-Notch-1*. Transcripts for *X-Delta-1* were found in presumptive neural tissues shortly after gastrulation. At neural plate stages, *X-Delta-1* is expressed in a distinct ring around the posterior end and in the lateral and medial neural plate (Fig. 1A), and later in the presumptive forebrain, midbrain, hindbrain, and spinal cord throughout neurula stages (Fig. 1B). Expression is also observed in the pronephros from neurula stages until swimming tadpole stages (Fig. 1B-E), and also in discrete points in the lateral epidermis, which may be post-migratory neural crest cells (Fig. 1F). Histological analysis shows that X-Delta-1 mRNA is present in the brain and the neural tube/spinal cord during neurula stages (Fig. 2). Expression narrows from the entire brain and neural tube during neurula stages to the periventricular zone and the regions adjacent to the central canal in the brain and spinal cord at swimming tadpole stages (Fig. 5B-F). In magnified images of the neural tube and spinal cord, *X-Delta-1* expression is observed in discrete points until swimming tadpole stages (Fig. 5A-F).

X-Notch-1 Expression

Antisense X-Notch ICD probes were used to determine the expression of *X-Notch-1*. X-Notch-ICD mRNA was detected in the neural folds after gastrulation, and neural expression continues in the forebrain, midbrain, hindbrain, eye, and spinal cord through swimming tadpole stages (Fig. 3). Histological analysis shows that *X-Notch-ICD* transcripts are present in the same tissues as *X-Delta-1* (Fig. 4), but magnification shows

that *X-Notch-1* is expressed diffusely throughout the brain and neural tube/spinal cord (Fig. 5G-L), in contrast to the dense points of *X-Delta-1* expression. At swimming tadpole stages expression of *X-Notch-1* is limited to the periventricular zone and the region adjacent to the central canal, similar to *X-Delta-1* (Fig. 5G-L). These expression patterns are consistent with X-Delta-1 acting as ligand and X-Notch-1 acting as receptor, since X-Delta-1 is in discrete points and X-Notch-1 appears diffuse in the same tissues. Additionally, at swimming tadpole stages X-Delta-1 and X-Notch-1 mRNA was detected in the regions around the periventricular zone and the central canal, which are sites of neurogenesis, suggesting that Notch signaling may regulate later cell fate decisions in the brain and spinal cord.

Effects of Notch Pathway Activation

The Notch signaling pathway was upregulated by injection of sense mRNA for X-Notch ICD into one blastomere of two-cell stage embryos, along with GFP mRNA as a tracer, and *in situ* hybridization was performed with antisense probes for *xNBT*, *xVGlut1*, and *xGAT1* to determine the effects of Notch signaling on neuronal, glutamatergic, and GABAergic phenotypes. Vehicle-injected control embryos were injected with water and GFP mRNA to determine if the microinjections were having any effect. Vehicle-injected embryos did not show any morphological defects or changes in expression of *xNBT*, *xGAT1*, or *xVGlut1* compared to non-injected controls (Fig. 6, Table 1). 56% of all X-Notch ICD-injected embryos showed gross morphological defects at swimming tadpole stages, including 21% in which the neural tube failed to close (Table 1, Fig. 6C, G, K). Expression of *xNBT* was generally similar in both lateral sides of the separated spinal

cord (Figs. 6C, 7C'). *xGAT1* was reduced on the injected side of 7/18 embryos, and

xVGlut1 was similarly reduced in 4/17 embryos (Table 1, Figs. 6K, 7K'). Cells that

expressed *xGAT1* and *xVGlut1* were spaced further apart from each other and were

observed over a wider area (Fig. 7G', K'). Expression of *xNBT*, *xGAT1*, or *xVGlut1* in

some cases was not clearly increased or decreased (Fig. 6G), but in other cases

expression was clearly absent in some regions of the spinal cord (Fig. 6K).

The morphologies of embryos with neural tube defects complicated bilateral

histological comparison of injected and uninjected sides. Sections of embryos with neural

tube defects are not shown. Histological analysis of embryos with less severely altered

morphology show that expression of *xNBT*, *xGAT1*, and *xVGlut1* is preserved on the

injected side of the embryo (Fig. 8B, C, E).

Effects of Notch Pathway Inhibition

The Notch pathway was inhibited by injecting mRNA for a dominant negative

form of xSu(H) into one blastomere of two cell stage embryos, and *in situ* hybridization

with the markers described previously was performed to determine the effects of

inhibited Notch signaling on neuronal, glutamatergic, and GABAergic phenotypes.

Embryos injected with xSu(H) DBM also had gross morphological defects at swimming

tadpole stages (64%) but had fewer neural tube defects (7.6%, Table 1). The neural tube

defects that were observed in xSu(H) DBM injected embryos were less pronounced than

those observed in X-Notch ICD injected embryos. Ectopic expression of *xNBT* and

xVGlut1 was observed outside of the normal regions of expression observed in control

embryos (Fig. 6D, L), and while no ectopic expression of *xGAT1* was observed, the

expression pattern was disorganized and over a wider region compared to controls (Fig. 6H). Ectopic expression of *xNBT* was observed on the injected side of the embryo as early as mid neurula stages (Fig. 9B). Additionally, assays for dopaminergic, serotonergic, and cholinergic neurotransmitter phenotype markers (xTh, xSert, xChat, respectively) showed that these neurotransmitter phenotypes were not affected (Fig. 10C, F, I).

Ectopic expression of *xNBT* and *xVGlut1* can also be observed in transverse sections (Fig. 9 E, G). Higher magnification shows that ectopic cells that express *xVGlut1* and *xNBT* are located at the epidermis and are several cell layers deep (Fig. 9F, H). The majority of cells that ectopically express *xNBT* also express *xVGlut1*, but expression does not overlap entirely, suggesting that some cells that ectopically express *xNBT* may be incompletely differentiated neurons that have not acquired a neurotransmitter phenotype (Fig. 10.2J, K). All cells that express *xVGlut1* also express *xNBT*.

Identity of Cells that Ectopically Express xNBT and xVGlut1

In order to determine the identity of the cells that ectopically express *xNBT* and *xVGlut1*, assays for *HNK-1*, *xVim*, and *xSlug* were performed. The cell surface protein HNK-1 is expressed on neural crest cells and the cell bodies and processes of primary neurons. Immunohistochemistry with HNK-1 was performed to determine if cells that ectopically expressed *xNBT* were also morphologically distinct neural cells. The assay for HNK-1 protein revealed ectopic expression in a similar pattern to *xVGlut1* and *xNBT* ectopic expression, suggesting that cells that ectopically express *xNBT* are *xVGlut1* are morphologically distinct neural cells with recognizable processes (Fig. 11C, D, E) that

are aberrant and disorganized (Fig. 11C, C'). In one observed embryo, expression of HNK-1 in the spinal cord was weaker on the injected side compared to the uninjected side, and small points of expression on the dorsal spinal cord, which may be cell bodies, were missing on the injected side (Figure 11D').

The cells that ectopically express *xNBT* and *xVGlut1* do not appear to be glial cells, nor do they appear to be derived from the neural crest. *XVim* encodes an intermediate filament protein that is expressed in radial glia (Dent et al., 1989) and perhaps other glial cell types in the spinal cord, intermyotomal spaces, and in a lateral line ventral to the somites (Fig. 12A). Expression of *xVim* is either ablated or disorganized beyond recognition on the injected side of xSu(H) DBM-injected embryos (Fig. 12B, D). Disorganized expression occurs mostly in the area of the spinal cord, and it is unclear if these injected embryos form myotomes correctly. Double *in situ* hybridization showed that cells that ectopically express *xVGlut1* did not also express neural crest marker *xSlug* (Fig. 12.2F, G), suggesting that the ectopic cells were not derived from the neural crest.

Effects of Inducible Constructs

Control embryos were injected with either X-Notch ICD-GR or xSu(H) DBM-GR and activated with the ligand dexamethasone at different times during gastrulation to determine the time periods in which altered Notch signaling would effect expression of *xNBT*, *xVGlut1*, or *xGAT1*. Injected embryos that were not induced with dexamethasone served as controls and were morphologically normal with unaltered expression of *xNBT* when assayed at late swimming tadpole stages (Fig. 12 A, B). Baseline comparisons to

X-Notch ICD-injected embryos suggest that the ICD-GR construct does not function as expected. Embryos that were treated with the ligand dexamethasone either two hours after injection or just prior to stage 10 were intended to be a baseline comparison to the constitutive X-Notch ICD construct, since the inducible construct would be activated well before endogenous expression of X-Notch ICD began. All embryos that were injected with X-Notch ICD-GR and activated with dexamethasone early, before stage 10, and at stage 11 or 13, developed normally and showed no morphological defects through later swimming tadpole stages (Fig. 13B). The identity of X-Notch ICD-GR plasmid DNA from which sense mRNA was transcribed has been confirmed by sequencing, and previous publications report that X-Notch ICD-GR produces effects similar to X-Notch ICD injections, so the reason for the inefficacy of xNotch ICD-GR remains unclear.

Activation of inducible xSu(H) DBM-GR prior to stage 10 resulted in morphological differences in 47% of analyzed embryos (Table 5). However, these morphological differences were not similar to those observed in xSu(H) DBM-injected embryos: 34% of embryos analyzed showed neural tube closure defects similar to those observed in constitutive X-Notch ICD-GR.

Expression of *xNBT* was also reduced in embryos injected with of xSu(H) DBM-GR and induced at stage 10, 11, and 13 (Fig. 13E-H). The magnitude of the effect is less in embryos activated at stage 13 than at stage 11, indicating that activation during different times of gastrulation has different effects. Nearly all embryos with reduced expression still showed *xNBT* expression in the forebrain and a few unidentifiable cranial nerves on the injected side (Fig. 13F-G). Embryos with reduced expression of *xNBT* often also had neural tube or other gross morphological defects, and it is unclear if expression

of *xNBT* was actually being reduced, or if the apparent effect was attributable to the gross morphological changes. In groups treated at stage 10 and 11, four total embryos were observed that showed bilateral expression of *xNBT* but had a highly rotated spinal cord, such that when the embryo lay on the opposite lateral side and most the midbrain, hindbrain, and spinal cord were not visible. However, three embryos were observed in the same groups that clearly had reduced or absent *xNBT* expression in the regions where the midbrain, hindbrain, and spinal cord normally were.

The high incidence of neural tube defects and the similarity in decreased expression of a neuronal marker suggests that this construct may actually be X-Notch ICD-GR. Comparison of supposed xSu(H) DBM-GR mRNA and X-Notch ICD-GR mRNA sizes by gel electrophoresis showed that the relative sizes were correct, indicating that the constructs had not been switched with each other. An alternate possibility is that xSu(H) DBM-GR was inadvertently switched for xSu(H) VP16, an active form of xSu(H) that is similar in size.

Discussion

Constitutively Active Notch Signaling does not Instruct GABAergic or Glutamatergic Fates

We hypothesized that Notch signaling regulates later cell fate decisions in neurogenesis, and the expression patterns of *X-Delta-1* and *X-Notch-1* support this hypothesis. Expression of the ligand *X-Delta-1* appears in discrete points in the spinal cord and *X-Notch-1* is expressed more diffusely in the same tissue, which is consistent with previously reported expression patterns in *Xenopus* (Coffman *et al.,* 1990; Chitnis *et al.,* 1995). Expression of the signaling pathway components was observed in sites of neurogenesis: the periventricular zone and the regions around the central canal in the spinal cord. Additionally, *X-Delta-1* mRNA was detected in small points in the epidermis, which may be post-migratory neural crest cells that form the peripheral nervous system.

However, while Notch signaling appears to have a role in neural development and possibly neurotransmitter phenotype specification, our data do not support our hypothesis that Notch signaling functions as a bimodal switch between programs for GABAergic and glutamatergic phenotypes. Notch activation resulted in disorganization of neurons, which is consistent with earlier findings that active Notch decreases the number of dopaminergic neurons in the spinal cord in *Xenopus* (Binor and Heathcote, 2005). It does not appear, however, that active Notch conversely acts instructively to specify either a GABAergic or glutamatergic phenotype. The authors of the *Xenopus* paper report that active Notch increases the spacing between dopaminergic neurons, and the same effect on GABAergic and glutamatergic neurons was observed here. Additionally, we observed

that expression of *xGAT1* and *xVGlut1* was absent from entire regions of the spinal cord, which is consistent with the standard model of Notch signaling, in which active Notch inhibits neurogenesis (reviewed in Louvi and Artavani-Tsakonas, 2006). No differential effect, however, was observed between GABAergic and glutamatergic phenotypes, indicating that Notch signaling does not act instructively in the decision between GABAergic and glutamatergic fates.

Notch Signaling may Restrict Glutamatergic Phenotypes

Our data suggest that Notch may act restrictively in the decision between GABAergic and glutamatergic fates, since inhibition of Notch signaling resulted in ectopic expression of *xVGlut1* and not *xGAT1*. However, a role for Notch regulating the number of GABAergic cells by limiting the number of glutamatergic cells is unclear, since expression of *xGAT1* in the spinal cord was not clearly reduced. Ectopic expression of *xNBT* similar to the ectopic expression observed here has been reported when proneural genes such as Xath3, Neurogenin, and NeuroD were overexpressed (Ma *et al.,* 1996; Perron *et al.,* 1999). This finding is consistent with the proposed model of *Xenopus* Notch signaling, in which Notch inhibits the expression of neurogenin (*Xngnr-1*) and prevents neuronal differentiation (Wettstein *et al.,* 1997). In the absence of Notch signaling, *Xngnr-1* is expressed at high levels and activates pro-neural genes, leading to ectopic expression of the neuron-specific filament protein *xNBT*.

Here we showed that most cells that ectopically expressed *xNBT* also expressed *xVGlut1*, indicating that the ectopic cells were glutamatergic. This result suggests that the cells that ectopically express neuronal markers when pro-neural genes are overexpressed

may also have a glutamatergic phenotype. While not all ectopic cells co-expressed *xNBT* and *xVGlut1*, no other neurotransmitter phenotype marker was ectopically expressed, suggesting that the glutamatergic phenotype exclusively is induced in ectopic cells, and that the remaining *xNBT* cells may be undifferentiated. This result is consistent with previous findings in which *X-ngnr-1* and *Xath3* overexpression resulted in ectopic expression of sensory neuron markers such as *xHox11L2* (Perron *et al.,* 1999), because one of the cell types that *xHox11L2* marks is glutamatergic Rohon-Beard neurons.

The finding that inhibition of Notch signaling results in ectopic expression of *xVGlut1* and not *xGAT1* is in opposition to our prediction that inhibition of Notch signaling would result in an increase in GABAergic neurons, since blocking Notch signaling in human neural stem cells resulted in predominantly GABAergic differentiation (Kabos *et al.,* 2002). This disagreement could be explained by the difference between organisms, but more likely it is due to the fact that cells that are cultured *in vitro* are not exposed to the signaling cues that occur *in vivo*. Moreover, in the human stem cell experiment Notch signaling was inhibited by blocking Hes-1, which is further downstream in the pathway.

Our finding suggests that the earliest neurotransmitter phenotype specified in *Xenopus* may be the glutamatergic phenotype; we expect that whichever phenotype is induced by Notch inhibition corresponds to the earliest phenotype that is induced, since presumptive neurons are not delayed from differentiating when Notch signaling is inhibited.

Ectopic Cells may be Related to Rohon-Beard Sensory Neurons

A positive identity for the cells that ectopically express *xNBT* and *xVGlut1* has not been established. It was unclear if the cells were fully differentiated neurons, since not all *xNBT*-expressing cells also expressed *xVGlut1*, and no other neurotransmitter phenotypes were ectopically expressed, suggesting that the remaining cells may have been undifferentiated. To address this issue, we performed immunohistochemistry with antibodies against HNK-1, which labels cell bodies and processes of primary neurons, enabling them to be visualized (Nordlander, 1993). We found that HNK-1 was ectopically expressed in what appeared to be aberrant processes of morphologically distinct neural cells. In addition to being located on primary neurons, HNK-1 is also normally expressed in the neurons and glia of the peripheral nervous system, which appear on the uninjected side of our embryos as points embedded in the epidermis. These discrete points were replaced with wide splotches of expression and thick, tangled processes on the injected sides of experimental embryos, suggesting that ectopic expression of *xNBT* may have been caused by increased induction of neural crest-derived peripheral neurons.

We performed double *in situ* hybridization with *xVGlut1* and neural crest marker *xSlug* to determine if ectopic expression was caused by aberrant growth of peripheral neurons. Peripheral neurons are derived from neural crest cells, and *xSlug* is a neural crest lineage marker (Mayor *et al.,* 1995). Cells that ectopically expressed *xVGlut1* did not also express the neural crest marker *xSlug*, indicating that the ectopic cells were not derived from neural crest cells. However, this does not completely eliminate the possibility that these cells were derived from the neural crest, since the expression of *xSlug* may have

been terminated in these cells. *XSlug* expression terminates as the embryo matures, and by swimming tadpole stages *xSlug* is only expressed in the posterior section of the spinal cord (data not shown). While *xSlug* is clearly expressed in the neural crest stem cells that are dorsal to the neural tube when the assay was performed at early tailbud stages, its expression may have been terminated in the post-migratory cells, which may have already differentiated.

Since the ectopic cells did not appear to be migratory neural crest cells, their location suggested that they may instead be ectopically induced primary neurons that were originally fated for epidermal or non-neuronal fates. Since the majority of these cells expressed *xVGlut1* and showed HNK-1 immunoreactivity, these cells may be developmentally related to Rohon-Beard neurons. Rohon-Beard neurons are an attractive possibility because they are glutamatergic primary neurons that are among the earliest neurons born (Lamborghini, 1980), and again cells that are induced as a result of Notch inhibition would be expected to display the phenotypes.

The hypothesis that these cells may have Rohon-Beard characteristics is consistent with results in zebrafish, where Notch signaling at the boundary of the neural plate limits the number of Rohon-Beard neurons that form (Cornell and Eisen, 2000). When Notch signaling is inhibited in zebrafish, supernumerary Rohon-Beard neurons form, with a concomitant decrease in neural crest cells. Our results are consistent with the findings in zebrafish, since Notch inhibition resulted in an increased number of what may be Rohon-Beard-like neurons. However, no ectopic expression of neurons was reported in zebrafish, suggesting either that Notch signaling behaves slightly differently in

zebrafish, or that we are observing the more dramatic effects due to the greater amount of experimental mRNA that we are injecting.

Since no known marker is exclusively expressed in Rohon-Beard neurons, a positive identification of ectopic cells as Rohon-Beard neurons may not be possible, since they are not located in the dorsal spinal cord. The establishment of any specific identity in ectopically induced cells is complicated by the fact that the cells are not expressed in a location where neurons typically are, and location is an essential aspect of identity. The expression of *xNBT, xVGlut1,* and *HNK-1* indicates that the cells could also be related to types of spinal cord interneurons or cells from the cranial nerves.

The lack of organization in the apparent processes of ectopic cells is consistent with the idea that axon growth and guidance is closely linked to both neurotransmitter phenotype specification programs and location (Gordidis and Brunet, 1999). Since the inhibition of Notch signaling may be inducing the program for glutamatergic differentiation in otherwise non-neuronal cells, it may also interfere with axon growth and guidance programs. Additionally, since the apparent neurons form outside of the normal regions of neuronal expression, they are not exposed to the normal chemoattractant and chemorepellent cues that guide axonal growth cones.

In one embryo in which Notch was inhibited, the expression of HNK-1 within the spinal cord appeared to be significantly decreased. Expression of the longitudinal column of HNK-1 immunoreactivity that runs from anterior to posterior in normal embryos are the processes of spinal cord neurons, which are organized into longitudinal columns (Roberts, 2000). On the injected side of the embryo, this longitudinal column was not as tightly organized, and expression of HNK-1 was reduced, suggesting that fewer processes

were in the column. Additionally, expression of HNK-1 was observed in discrete points in the spinal cord on the uninjected side, but these points were absent on the injected side. These points are most consistent with the appearance of Rohon-Beard neurons in zebrafish (Cornell and Eisen, 2000), but they could also be the cell bodies of other spinal cord neurons. If these are in fact the cell bodies of Rohon-Beard neurons, then it would seem that the inhibition of Notch signaling inhibited their formation in the spinal cord, which would disagree with the effect of Notch signaling inhibition in zebrafish. More embryos of this particular phenotype, which may have been the result of the delivery of less xSu(H) DBM mRNA, need to be analyzed to determine if this phenotype is commonly reproduced.

Since it was unclear whether the morphologically distinct cells that showed HNK-1 immunoreactivity were neurons or glia, Vimentin (xVim) expression was determined in embryos with inhibited Notch signaling. *XVim* expression was reduced on the injected side of embryos, suggesting that glial cells were not ectopically induced and that the normal expression of *xVim* was disrupted by the inhibition of Notch signaling. This result fits the paradigm in which active Notch promotes gliogenesis, since many glial cells appear to have been lost when Notch signaling was inhibited (Morrison *et al.,* 2002). This result suggests that ectopic cells are induced at the cost of radial glia, possibly by causing multipotent progenitor cells, which would normally give rise to radial glia, to differentiate into neurons instead. More assays, however, are necessary to determine if all types of glial cells are reduced in embryos that show ectopic expression of neuronal markers.

Future Directions

While our hypothesis was not supported because active Notch decreased both glutamatergic and GABAergic marker expression, it is possible that Notch regulates decisions between neurotransmitter phenotype later in development, a hypothesis supported by the expression of *X-Notch-1* and *X-Delta-1* in the spinal cord through swimming tadpole stages. An effective method for delaying the activity of X-Notch-ICD and xSu(H) DBM needs to be established to determine if later episodes of Notch signaling affect neurotransmitter phenotype specification. It is unclear why different effects are observed between constitutive Notch inhibition and inducible Notch inhibition in cases of baseline comparison. It is also unclear why inducible X-Notch ICD-GR activation does not have any apparent effects, as this construct has been previously reported to act similarly to constitutive Notch when activated (Contakos *et al.,* 2005; McLaughlin *et al.,* 2000). Our procedure for using the inducible constructs needs to be modified in a way that ensures the proteins are having an effect, and if this proves unsuccessful alternate inducible constructs for other components of the Notch signaling pathway could possibly be obtained.

A functional inducible construct of xSu(H) DBM would be essential to understanding the time frame in which ectopic expression of *xNBT* and *xVGlut1* could be induced. Knowing when ectopic expression is potentially induced would move toward understanding the origin of the ectopic cells, since it could be determined if they were induced during primary neural induction from the non-neural ectoderm or later during neural plate stages from cells that were fated to be neural crest.

Our results lead us to ask what the identity of the cells that ectopically express *xNBT* and *xVGlut1* is, and assays for a later marker of post-migratory neural crest cells and for markers of other types of glial cells need to be performed to determine this. While it may not be possible to completely ascertain an identity for the ectopic cells because of their location, it is possible to narrow down the possibilities in order to gain a better understanding of the effects of Notch inhibition on the specification of neural crest and glial fates.

The results of assays for HNK-1 protein suggest that lower doses of injected constructs need to be administered to determine any dose-dependent effects, since the one embryo in which spinal cord cell bodies were absent also showed less pronounced ectopic expression. It would also be of interest to determine if the severity of neural tube defects and the extent of decreased neuronal specification observed as a result of X-Notch ICD injections would be lessened by delivery of less mRNA.

The most promising aspect of the results we obtained with constitutive Notch inhibition is the possible application to answering questions about the earliest neurotransmitter phenotypes that are specified. Overexpression of pro-neural genes causes ectopic expression neuron-specific filament proteins and sensory neuron markers (Perron *et al.,* 1999), but a neurotransmitter phenotype for these ectopic cells had not been reported previously, and our results suggest that these ectopic cells may be glutamatergic, and may additionally share properties with Rohon-Beard neurons. The role of Notch in inhibiting proneural genes suggests that the ectopic cells that are induced by Notch inhibition and the ones induced by overexpression of proneural genes are the result of the same process. Assays for *xVGlut1* could be performed in embryos in which Xngnr-

1, Xash-3, or NeuroD were overexpressed to determine if the resultant ectopic neurons are predominantly glutamatergic, which would make a strong case for the glutamatergic phenotype as the "default" or earliest neurotransmitter that is specified. Additional experiments to determine the nature of ectopic cells could elucidate not only details of the effects of the Notch signaling pathway, but the characteristics of the developmental programs that specify of the earliest neurotransmitter phenotypes as well.

Other components of the pathway need to be studied for their role in neurotransmitter phenotype specification. There are three Notch receptors in *Xenopus tropicalis* (Theodosiou *et al.,* 2009), and additional ligands too. The ligand X-Delta-2 is also involved in neurogenesis, eye development, and the segregation of the hindbrain (Peres and Durston, 2006), and X-Serrate, another ligand to the Notch receptor, is involved in neurogenesis as well (Kiyota and Kinoshita, 2004). The multiple roles of xSu(H) need to be determined as well, since xSu(H) may be an integral part of the PTF-1 transcription factor complex, which drives GABAergic differentiation in the retina (Dullin *et al.,* 2007). Moreover, the pathways of Wnt signaling and Notch signaling interact in some cell fate decisions, and may do so during neurogenesis as well (Cheng *et al.,* 2008). The Notch signaling pathway is still a promising candidate for the regulation neurotransmitter phenotype specification, and its many ligands, receptors, and effectors indicate that the full range of its effects are poorly understood.

Notch signaling may also interact with calcium activity, which has been proposed as a means of specifying neurotransmitter phenotype (Gu and Spitzer, 1997). Cells of the *Xenopus* spinal cord show fluctuations in concentration of intracellular calcium, and the patterns of this calcium activity have been linked to specific neurotransmitter phenotypes.

Since changes in intracellular calcium are most likely effected by calcium channels, it is a possibility that one of the effects of Notch signaling is to alter the expression of these channels. Research on the effects of Notch signaling on the expression of calcium channels could elucidate interactions between proposed mechanisms and may reveal an integrated mechanism for the differential cell type specification of neighboring cells.

References

Artavanis-Tsakonas, S., M. D. Rand, et al. (1999). "Notch signaling: cell fate control and signal integration in development." Science **284**(5415): 770-6.

Barembaum, M. and M. Bronner-Fraser (2005). "Early steps in neural crest specification." Semin Cell Dev Biol **16**(6): 642-6.

Beatus, P. and U. Lendahl (1998). "Notch and neurogenesis." J Neurosci Res **54**(2): 125-36.

Binor, E. and R. D. Heathcote (2005). "Activated notch disrupts the initial patterning of dopaminergic spinal cord neurons." Dev Neurosci **27**(5): 306-12.

Briscoe, J. and B. G. Novitch (2008). "Regulatory pathways linking progenitor patterning, cell fates and neurogenesis in the ventral neural tube." Philos Trans R Soc Lond B Biol Sci **363**(1489): 57-70.

Bronner-Fraser, M. and S. E. Fraser (1988). "Cell lineage analysis reveals multipotency of some avian neural crest cells." Nature **335**(6186): 161-4.

Cheng, X., T. L. Huber, et al. (2008). "Numb mediates the interaction between Wnt and Notch to modulate primitive erythropoietic specification from the hemangioblast." Development **135**(20): 3447-58.

Chitnis, A., D. Henrique, et al. (1995). "Primary neurogenesis in Xenopus embryos regulated by a homologue of the Drosophila neurogenic gene Delta." Nature **375**(6534): 761-6.

Chitnis, A. B. (1999). "Control of neurogenesis--lessons from frogs, fish and flies." Curr Opin Neurobiol **9**(1): 18-25.

Coffman, C., W. Harris, et al. (1990). "Xotch, the Xenopus homolog of Drosophila notch." Science **249**(4975): 1438-41.

Coffman, C. R., P. Skoglund, et al. (1993). "Expression of an extracellular deletion of Xotch diverts cell fate in Xenopus embryos." Cell **73**(4): 659-71.

Contakos, S. P., C. M. Gaydos, et al. (2005). "Subdividing the embryo: a role for Notch signaling during germ layer patterning in Xenopus laevis." Dev Biol **288**(1): 294-307.

Cornell, R. A. and J. S. Eisen (2000). "Delta signaling mediates segregation of neural crest and spinal sensory neurons from zebrafish lateral neural plate." Development **127**(13): 2873-82.

Cornell, R. A. and J. S. Eisen (2002). "Delta/Notch signaling promotes formation of zebrafish neural crest by repressing Neurogenin 1 function." Development **129**(11): 2639-48.

De Robertis, E. M. and H. Kuroda (2004). "Dorsal-ventral patterning and neural induction in Xenopus embryos." Annu Rev Cell Dev Biol **20**: 285-308.

Dent, J. A., A. G. Polson, et al. (1989). "A whole-mount immunocytochemical analysis of the expression of the intermediate filament protein vimentin in Xenopus." Development **105**(1): 61-74.

Doe, C. Q. and C. S. Goodman (1985). "Early events in insect neurogenesis. II. The role of cell interactions and cell lineage in the determination of neuronal precursor cells." Dev Biol **111**(1): 206-19.

Dullin, J. P., M. Locker, et al. (2007). "Ptf1a triggers GABAergic neuronal cell fates in the retina." BMC Dev Biol **7**: 110.

Ellisen, L. W., J. Bird, et al. (1991). "TAN-1, the human homolog of the Drosophila notch gene, is broken by chromosomal translocations in T lymphoblastic neoplasms." Cell **66**(4): 649-61.

Goridis, C. and J. F. Brunet (1999). "Transcriptional control of neurotransmitter phenotype." Curr Opin Neurobiol **9**(1): 47-53.

Goridis, C. and H. Rohrer (2002). "Specification of catecholaminergic and serotonergic neurons." Nat Rev Neurosci **3**(7): 531-41.

Gu, X. and N. C. Spitzer (1997). "Breaking the code: regulation of neuronal differentiation by spontaneous calcium transients." Dev Neurosci **19**(1): 33-41.

Harland, R. (2000). "Neural induction." Curr Opin Genet Dev **10**(4): 357-62.

Harris, W. A. and V. Hartenstein (1991). "Neuronal determination without cell division in Xenopus embryos." Neuron **6**(4): 499-515.

Heathcote, R. D. and A. Chen (1993). "A nonrandom interneuronal pattern in the developing frog spinal cord." J Comp Neurol **328**(3): 437-48.

Heathcote, R. D. and A. Chen (1994). "Morphogenesis of catecholaminergic interneurons in the frog spinal cord." J Comp Neurol **342**(1): 57-68.

Kabos, P., A. Kabosova, et al. (2002). "Blocking HES1 expression initiates GABAergic differentiation and induces the expression of p21(CIP1/WAF1) in human neural stem cells." J Biol Chem **277**(11): 8763-6.

Kiyota, T. and T. Kinoshita (2004). "The intracellular domain of X-Serrate-1 is cleaved and suppresses primary neurogenesis in Xenopus laevis." <u>Mech Dev</u> **121**(6): 573-85.

Kos, R., M. V. Reedy, et al. (2001). "The winged-helix transcription factor FoxD3 is important for establishing the neural crest lineage and repressing melanogenesis in avian embryos." <u>Development</u> **128**(8): 1467-79.

Kos, R., M. V. Reedy, et al. (2001). "The winged-helix transcription factor FoxD3 is important for establishing the neural crest lineage and repressing melanogenesis in avian embryos." <u>Development</u> **128**(8): 1467-79.

Lamborghini, J. E. (1980). "Rohon-beard cells and other large neurons in Xenopus embryos originate during gastrulation." <u>J Comp Neurol</u> **189**(2): 323-33.

Leclerc, C., I. Neant, et al. (2006). "Calcium transients and calcium signalling during early neurogenesis in the amphibian embryo Xenopus laevis." <u>Biochim Biophys Acta</u> **1763**(11): 1184-91.

Lee, J. E., S. M. Hollenberg, et al. (1995). "Conversion of Xenopus ectoderm into neurons by NeuroD, a basic helix-loop-helix protein." <u>Science</u> **268**(5212): 836-44.

Li, L., I. D. Krantz, et al. (1997). "Alagille syndrome is caused by mutations in human Jagged1, which encodes a ligand for Notch1." <u>Nat Genet</u> **16**(3): 243-51.

Louvi, A. and S. Artavanis-Tsakonas (2006). "Notch signalling in vertebrate neural development." <u>Nat Rev Neurosci</u> **7**(2): 93-102.

Ma, Q., C. Kintner, et al. (1996). "Identification of neurogenin, a vertebrate neuronal determination gene." <u>Cell</u> **87**(1): 43-52.

Mayor, R., R. Morgan, et al. (1995). "Induction of the prospective neural crest of Xenopus." <u>Development</u> **121**(3): 767-77.

Messenger, N. J. and A. E. Warner (1989). "The appearance of neural and glial cell markers during early development of the nervous system in the amphibian embryo." <u>Development</u> **107**(1): 43-54.

Morrison, S. J., S. E. Perez, et al. (2000). "Transient Notch activation initiates an irreversible switch from neurogenesis to gliogenesis by neural crest stem cells." <u>Cell</u> **101**(5): 499-510.

Nordlander, R. H. (1993). "Cellular and subcellular distribution of HNK-1 immunoreactivity in the neural tube of Xenopus." <u>J Comp Neurol</u> **335**(4): 538-51.

Peres, J. N. and A. J. Durston (2006). "Role of X-Delta-2 in the early neural development of Xenopus laevis." <u>Dev Dyn</u> **235**(3): 802-10.

Perron, M., K. Opdecamp, et al. (1999). "X-ngnr-1 and Xath3 promote ectopic expression of sensory neuron markers in the neurula ectoderm and have distinct inducing properties in the retina." <u>Proc Natl Acad Sci U S A</u> **96**(26): 14996-5001.

Poulson, D. (1940)." The effects of certain X-chromosome deficiencies on the embryonic development of *Drosophila Melanogaster*." <u>J. Exp. Zool</u>. **83**, 271-325.

Roberts, A. (2000). "Early functional organization of spinal neurons in developing lower vertebrates." <u>Brain Res Bull</u> **53**(5): 585-93.

Sambrook, J., Russel, D.W., 2001. Molecular Cloning: A Laboratory Manual, third ed. Cold Spring Harbor Laboratory Press, Cold Spring Harbor, New York.

Nieuwkoop, P.D., Faber, J., 1994. Normal Table of *Xenopus laevis* (Daudin). Garland Publishing, New York.

Sasai, Y. (1998). "Identifying the missing links: genes that connect neural induction and primary neurogenesis in vertebrate embryos." <u>Neuron</u> **21**(3): 455-8.

Sasai, Y., M. Ogushi, et al. (2008). "Bridging the gap from frog research to human therapy: a tale of neural differentiation in Xenopus animal caps and human pluripotent cells." <u>Dev Growth Differ</u> **50 Suppl 1**: S47-55.

Sive, H.L, Grainger, R.M., Harland, R.M., (2000). Early Development of *Xenopus laevis:* A Laboratory Manual. Cold Spring Harbor Laboratory Press, Cold Spring Harbor, New York.

Theodosiou, A., S. Arhondakis, et al. (2009). "Evolutionary scenarios of Notch proteins." <u>Mol Biol Evol</u>.

Tsai, M. Y., P. W. Wong, et al. (1997). "Identification of a splice site mutation in the cystathionine beta-synthase gene resulting in variable and novel splicing defects of pre-mRNA." <u>Biochem Mol Med</u> **61**(1): 9-15.

Weinstein, D. C. and A. Hemmati-Brivanlou (1999). "Neural induction." <u>Annu Rev Cell Dev Biol</u> **15**: 411-33.

Wettstein, D. A., D. L. Turner, et al. (1997). "The Xenopus homolog of Drosophila Suppressor of Hairless mediates Notch signaling during primary neurogenesis." <u>Development</u> **124**(3): 693-702.

Wharton, K. A., K. M. Johansen, et al. (1985). "Nucleotide sequence from the neurogenic locus notch implies a gene product that shares homology with proteins containing EGF-like repeats." Cell **43**(3 Pt 2): 567-81.